UNIVERSITY OF OKLAHOMA

GRADUATE COLLEGE

VIRTUAL MEASUREMENT OF VALVE PERFORMANCE AND ITS APPLICATION IN ENERGY EFFICIENCY IMPROVEMENTS

A THESIS

SUBMITTED TO THE GRADUATE FACULTY

in partial fulfillment of the requirements for the

Degree of

MASTER OF SCIENCE

By

SHIMA S. SHAHAHMADI
Norman, Oklahoma
2018

VIRTUAL MEASUREMENT OF VALVE PERFORMANCE
AND ITS APPLICATION IN ENERGY EFFICIENCY IMPROVEMENTS

A THESIS APPROVED FOR THE
SCHOOL OF AEROSPACE AND MECHANICAL ENGINEERING

BY

_____
Dr. Li Song, Chair

_____
Dr. Yingtao Liu

_____
Dr. Jie Cai

Acknowledgements

I would like to thank Dr. Song, my advisor, for providing tremendous help and support throughout my graduate studies at the University of Oklahoma. She was a great mentor to me. She helped me improve my understanding of the theoretical and practical aspects of heating, ventilation, and air-conditioning. She helped me engage in academic research in this topic. She introduced me to a global network of professionals in this area. And she helped me launch a career in this line of engineering. For all of these, I am grateful to her.

I would also like to thank Dr. Yingtao Liu and Dr. Jie Cai for reviewing my thesis and for giving me advice to improve the content and the presentation of this thesis. I am also thankful to the anonymous referees at *ASHRAE Transactions* for reviewing one of the chapters of this thesis, which is now published in their outlet. Lastly, I am grateful to the participants at many academic and professional conferences for their useful comments on the content of this thesis.

Table of Contents

List of Tables

List of Figures

Abstract

For heating, ventilation, and air-conditioning engineers, the measurement of system performance is a vital step in ensuring that the system in use is functioning at its optimal functionality. The measurement of water flow rate and the measurement of air flow rate are both among the key measurement efforts in this line of mechanical engineering. Traditionally, physical devices were used for this purpose. Increasingly, however, academic research is exploring the possibility of virtual flow measurement (e.g., Swamy, Song, and Wang 2012).

In practice, virtual measurement has many advantages over traditional measurements that use physical devices. Virtual meters are shown to be cost effective. Unlike physical meters, they do not require extra space, and they do not intervene with air or water flow. Also, if done properly, they are shown to be as accurate, when compared to physical meters.

This thesis explores the theoretical and the practical aspects of using virtual valve flow meters to monitor chilled water flow rate in modern systems that are used in a medical facility in Oklahoma City, OK. Virtual valve flow meters are measurement devices that make use of valve command information (available in building automation systems) and valve differential pressure data (recorded by physical differential pressure sensors) to measure the flow rate of a given valve without relying on any physical flow measurement devices that intervene with the flow rate, require a large space, or impose installation and maintenance cost. In particular, this thesis work tackles some practical challenges that negatively affect

the accuracy of virtual measurement of the valve flow meter. It examines the key problem that the valve commands do not necessarily reveal the accurate position of valve. Not only the changes in pressure across the valve matters for virtual measurement, but also the actual opening position of the valve matters. However, the information about valve commands are not necessarily a reliable source for identifying valve position.

It is argued that stiction/resolution and deadband are among the factors that cause the mis-match between valve command and valve position. Stiction is known as the static friction resistance to valve movement, and the actuator resolution is the smallest possible movement that an actuator can initiate. Also, deadband is known as the hysteresis in the reversal of valve movements. All of these may lead to a mis-match between system command and the physical positioning of the valve. Significant virtual measurement inaccuracy is caused by the above mis-match. To improve upon the accuracy, it is vital to examine valves' dynamic behavior through their characteristic curve. Incorporating stiction/resolution and deadband, a detailed understanding of this behavior enables the researcher to correct for the above mis-match. This correction requires two steps: first, when valve command changes are not large enough to overcome a particular threshold, valve positions should stay the same; second, when the reverse signal changes are not significant to overcome a particular threshold, valve position should again remain the same. These simple steps could be taken when the behavior of valve is fully examined.

Motivated by the possibility of these corrections, the theoretical foundations of improvement in virtual flow measurement is examined in this thesis. More

importantly, the application of this improved measurement method is examined for two different sizes of air handling units. The results confirm that the computation of valve dynamic behavior could significantly improve the accuracy of virtual flow meters. In order to show the application of these meters, this thesis also explores how virtual flow rate measurements could be used in assessing the performance of an industry-wide standard that leads to improving energy efficiency. In particular, using virtual meters, the study in this thesis has shown that customizing minimum airflow rate, as instructed by ASHRAE standard 90.1, could lead to significant energy savings in medical facilities.

Further research could be focused on exploring other factors that could affect the accuracy of virtual flow measurement. They could also be focused on testing the effectiveness of virtual valve flow measurement in other facilities, including commercial, and academic facilities. Future academic research in this topic could also be instrumental in generalizing and simplifying the virtual valve flow measurement procedures for application in HVAC industry. Most of the ongoing research has been limited to academic findings and proposals. There appears to be a disconnect between these findings and proposals and industry-application of virtual measurement. There is, in particular, a room for the design of an advanced device that incorporates the estimated coefficients from each air-handling unit's valve characteristic curve into the required computation for virtual flow measurement. This could, in future, facilitate the industrial application of virtual flow measurement.

Chapter 1: Introduction

Effective monitoring of mechanical and electrical systems heavily depends on precise measurements. Given the installation, maintenance, and costs of physical measurement devices and given their special requirements, engineers have recently turned to virtual measurements that could substitute for physical meters. Recent advancement in computational capacities have also made this trend more popular and effective.

Considering these developments, virtual flow measurement has increasingly become popular in monitoring the performance of Heating, Ventilation, and Air Conditioning (henceforth, HVAC) systems. In fact, as suggested by Song et al. (2013), it has already been about 15 years ever since the initial idea for employing virtual flow measurement was put forth. This was done in a study by Joo et al. (2003), in which a virtual fan airflow meter was used for the first time. Following that study, many researchers have made use of virtual flow measurements.

Against the backdrop of recent developments in virtual measurements, practical improvements in virtual water flow rate measurement are explored in this thesis. Following a description of the theoretical foundations of this measurement and some empirical assessment of its performance, an example for application of virtual measurement in monitoring the performance of modern HVAC systems is also provided and fully discussed.

To provide a background, recent developments in virtual measurement is discussed in Section 1.1. Practical challenges in system implementation are discussed in Section 1.2. Lastly, proposed solutions are briefly discussed in Section 1.3, and thesis layout is described.

1.1 Introduction of virtual meter development in HVAC industry

It is suggested by Song et al. (2012) that, though virtual measurement had already been used in other industries, one of the early experiments in using virtual measurement in HVAC industry was conducted by Lee and Dexter (2005) following the work by Joo et al. (2003). In their study, the temperature of the air that was leaving the mixing-box of an air handling unit (henceforth, AHU) was examined using a virtual temperature measurement algorithm. In practice, such measurement is vital in understanding the performance of the AHUs. Given the variations in temperature, however, this measurement always proves to be quite demanding. Using a model that relates the measured temperature to the average temperature of the air, a virtual temperature measurement algorithm was developed by Lee and Dexter (2005) to understand and control for the uncertainties that are involved in temperature measurement. Following the above study, it was shown by Wichman and Braun (2009) that, when it came to the air coming out of AHUs, measured mixed-air temperature could be augmented with a correlation for bias error that is a function of damper control signal, outdoor air, and return air temperature. Using this correlation and the bias correction that follows, it was illustrated by the authors that there was a significant improvement in air temperature measurement. This result is in line with the findings in Lee and Dexter

(2005), showing how the usage of virtual meter techniques could improve air temperature measurement.

Measurement of building cooling load using a hybrid method was also examined in Huang et al. (2008). In their study, the differential water temperature and water flow rate were used for direct measurement. Theoretical chiller models were also used in their work, employing the information about chiller electrical power input. It is shown that this hybrid approach may improve the measurement of cooling load in high-rise buildings.

A virtual pump water flow was examined in Andiroglu et al. (2016) using either the variable-frequency drive input power or motor input power with calibrated pump. In their study, the motor and variable-frequency drive efficiencies were examined. Also, the potential energy losses were considered. It is shown that virtual measurement has a relatively high coefficient of determination, when compared to physical meters. In a closely-related study, a virtual pump water flow meter was developed by Wang et al. (2016). In their study, motor efficiency was modeled empirically as a function of motor power and other factors using regression analyses. Also, a function was constructed for pump efficiency in their study using pump shaft power and head. Following this method, an experiment was conducted in Wang et al. (2016) that showed that virtual measurement could well be in line with physical measurement.

It was also shown in Cheung and Braun (2014) that virtual sensors could be used for measuring the performance of rooftop units and cooling capacity. The novelty of their study is in the usage of power transmitters and thermocouples in

"training" the virtual sensors. After temporary usage of power transmitters and thermocouples, it was suggested by the authors that virtual sensors could continue measuring the electrical consumption and cooling capacity via temperature measurements. Their proposed method was tested empirically in real sites and in laboratories.

Further, a virtual airflow meter was developed in Wang et al. (2014), employing a motor efficiency model (that projected motor efficiency under variable frequency and voltage) and an in-situ fan efficiency curve. Similar to their contribution, a virtual airflow sensor was later developed in Prieto et al. (2017) that made use of operational data and in-situ fan curves calibration to calculate airflow rate. In particular, a calibration procedure was developed in their work through minimizing the turbulence impact on the air velocity measurements, evaluating the velocity distribution profile across a traverse section, and developing a synchronized calibration between the supply air and return air fan. It was shown that velocity measurements over a longer period of time could improve the accuracy when the spatial traverse coverage is sacrificed. The results in Prieto et al. (2017) illustrates that in-situ fan curve calibration is crucial in precise virtual measurement.

Modern methods of measurement in HVAC systems are proposed in these studies. Also, many improvements are documented when these methods are followed. Two recent examples include Shahahmadi and Song (2018) and McDonald et al. (2014).

1.2 Virtual valve flow meter mechanism and its challenge in system implementation

When it comes to measurements that are implemented in modern HVAC systems, many devices could easily be connected to control systems to implement the desired measurements. Examples include temperature sensors, CO_2 sensor, or humidity sensor. Many other devices, however, may present practical challenges in system implementation. Examples include flow rate measurement devices, power meters, or velocity measurement devices. Typically, flow rate measurement devices are expensive or require long straight pipes/ducts, so academics and manufacturers turn to virtual flow measurement rather than utilizing physical devices. To conduct virtual measurement, several algorithms are developed that rely on data from other sensors that could easily be connected to the control system.

That said, there are many challenges in implementation of virtual measurement procedures. In particular, this thesis is focused on resolving one of the key challenges that exist in system implementation of virtual measurement of water flow rates in modern valves. The underlying practical challenge that is addressed in this thesis relates to a virtual valve flow meter that was developed by Song et al. (2013). For this virtual meter, valve commands are used to represent valve positions in flow calculations. However, this particular virtual measurement procedure was developed based on an assumption that the valve oscillated only over a short period of time. When hourly average data were used, it would have been safe to assume that potential differences between hourly-averaged valve commands and valve positions are eliminated. Despite this reasonable proposition, empirical

evidence revealed the shortcomings of hourly-averaged data, suggesting that valve command signals do not necessarily represent the physical positioning of the valve accurately. This was, in fact, evident when a valve experiences a slow opening or closing, but not oscillations. Shahahmadi and Song (2018) offer a detailed example. Under these circumstances, a correction procedure is required in order to successfully employ valve commands in virtual measurement. This correction is fully described in Chapter 2. Once the required correction is conducted, the information from corrected valve command could be used to provide a better-informed prediction of valve position. Such correction makes virtual measurement of valve water flow rates more precise and practical. A related experiment is fully discussed in Chapter 3.

The above-mentioned challenge is only one example. There are other challenges in implementing virtual measurement. A key factor, as discussed in later chapters, is the computational capacity of automation systems that are available in residential, medical, or commercial buildings. Sometimes virtual measurement may require heavy computations that would require additional devices. That may increase the cost, defeating the main purpose of virtual measurement. Those computational devices may be expensive, and they may require constant maintenance. Thus, it is of vital importance to develop virtual measurement systems that could rely on the existing computational capacities in modern automation and control systems.

1.3 Proposed solution and thesis layout

In this thesis, the usage of virtual flow measurement in modern HVAC systems is further examined. In particular, this thesis is focused on enhancements in virtual flow measurements applied to some of the HVAC control valves that are employed in HVAC systems. These enhancements are shown to be possible through a careful examination of the dynamic behavior of valves. A theoretical discussion of this topic is offered in Chapter 2, while an empirical exercise is described in Chapter 3.

For the empirical exercise, enhancement in virtual flow measurement through a careful examination of valve dynamic behavior is tested for using the data obtained from the operation of two AHUs that are installed in a large facility in Oklahoma City, OK. The AHUs that are examined vary in size. Yet, there are convincing evidence that in both cases computing valve dynamic behavior may in practice improve the precision of virtual flow measurement. This finding is, in particular, highlighted in Shahahmadi and Song (2018).

Given the illustrated use of virtual flow measurement, this thesis also explores how such measurements could help HVAC engineers to improve energy efficiency of AHUs through changes in Variable Air Volume (henceforth, VAV) settings. For this empirical exercise, discussed fully in Chapter 4, a recently revised guideline by the American Society of Heating, Refrigerating and Air-Conditioning Engineers is examined. Implementing this guideline (noted as ASHRAE Standard 90.1) leads to a reduction to 30% of maximum airflow for the VAVs; in particular, the VAVs that serve non-critical zones. As highlighted in Shahahmadi, Rivas, Song, and Wang (2017), virtual flow measurement could successfully be used for

the implementation of this revised guideline. In fact, it is shown that resetting the VAVs that leads to a reduction in supply fan speeds and supply air flow could translate into significant decline in cooling energy consumption.

The remainder of this thesis is organized in the following way. In Chapter 2, the theoretical backgrounds of improvements in virtual flow measurement using dynamic valve behavior is discussed. In doing so, the possibility of a mismatch between valve command and valve position and its effects on the precision of virtual flow measurements are described. This chapter concludes with describing an empirical approach to identifying and quantifying the sources of the above mismatch. In Chapter 3, the theoretical guidelines and the empirical approach that are introduced in Chapter 2 are put into work to measure the flow rate of a relatively small AHU and a relatively large AHU. The findings illustrate the advantages and shortcomings of virtual flow meters. In particular, the uncertainty analyses reveal how considering the dynamic behavior of the valves may improve the precision of virtual flow measurement. Given the usefulness of virtual flow measurement, as illustrated in Chapter 3, a case study is discussed in Chapter 4 that shows how virtual flow measurement could be used in evaluating the effectiveness of a revised guideline by ASHRAE. In particular, virtual flow measurement is used to show how adjusting the VAV settings may lower energy consumption through lowering supply fan speed and airflow. In Chapter 5 the above findings are summarized, and conclusions are drawn accordingly.

Chapter 2: Valve Flow Meter Enhancement Through Computing Valve Dynamic Behavior: A Theoretical Discussion

In this chapter, a method of valve virtual flow measurement improvement is discussed in detail. The objective of this discussion is to review the empirical method, developed in Shahahmadi and Song (2018), that could be used in order to improve the virtual flow measurement, considering the limited computational capacities in building automation systems. This empirical method will then be employed in the experiments that are described in the following chapters.

The concept of the valve virtual flow measurement is first described in Section 2.1. The possibility of a mismatch between valve command (i.e., controller input) and valve position (i.e., observed output) is then discussed in Section 2.2. It is also described how such mismatch may affect the precision of virtual flow measurement. Lastly, in Section 2.3, an empirical approach for identifying the sources of the above-mentioned mismatch is introduced.

2.1. Virtual Flow Measurement

Previous studies suggest that measurement of valve flow rate may in practice be quite challenging. In particular, the sensors that are installed in ducts or pipes may disrupt the flow rate, which in turn makes the measurement of the flow rate nonviable. This highlighted in Andiroglu (2015) and Wang et al. (2014), who argued that space and cost limitations might affect the implementation of physical flow measurement.

The ASHRAE Handbook (2013) provides an example of the demanding requirements for the installation of the physical flow rate meters. This handbook

suggests that physical meter installation is viable only when long, straight, and unobstructed pipes or ducts are available. Those pipes or ducts must be of 7.5 times over the pipe or duct diameter upstream and 3 times over the same diameter downstream in order for physical meters to measure the flow rate properly. These requirements along with the cost of physical flow meter devices may impede the installation of such devices in HVAC systems in residential, commercial, medical, or academic buildings.

As indicated in Song et al. (2013), the idea behind using a virtual flow meter was initially put forth about 15 years ago when the use of a virtual fan airflow meter was proposed by Joo et al. (2003). Tracking the supply air flow rate, a virtual meter is developed in their study to measure the supply and return air flow rate. In turn, employing this virtual flow rate measurement, it is suggested that fan power could be saved by resetting the static pressure set points.

Many studies, then, followed as summarized by Song et al. (2012). Among those studies, the use of valve dynamic behavior for virtual flow rate measurement was first discussed in Song et al. (2013). For a given AHU, the control valves are installed to control the flow rate of chilled or hot water through cooling or heating coils, respectively. The pressure drop across these valves could be used for the measurement of flow rate. For this purpose, pressure drop, valve opening position, and valve characteristic curve should be used in the following fashion:

$$Q_z = f_v(z)\sqrt{\Delta P_v} \tag{1}$$

In the above equation, Q_z is the flow rate, $f_v(z)$ is the *installed* valve characteristic curve for a given opening position of z, and ΔP_v is the differential pressure across the valve. The installed valve characteristic curve, as indicated in Song et al. (2013), is a function of a constant valve flow coefficient, valve's *inherent* characteristic, and valve authority. Given the details of valve design, the above parameters are known to us. Also, pressure differential is measurable. However, the actual valve opening position is unknown. Fortunately, valve command, which are available from the building automation systems, could be used to replace the unknown valve position. Therefore, the flow rate could empirically be measured using the following formula:

$$Q_x = f_v(x)\sqrt{\Delta P_v} \tag{2}$$

where Q_x is the calculated flow rate, $f_v(x)$ is the *installed* valve characteristic curve for the observed valve command x, and ΔP_v is the differential pressure across the valve.

2.2. The Mismatch Between Valve Command and Valve Position

The greatest advantage of the usage of virtual flow meters is that it does not require the installation of expensive physical flow meters that by design disrupt the water flow rate and occupy unnecessarily large spaces. In this approach, we would rather rely on the observed differential pressure, valve command, and valve characteristic curve. Nonetheless, this approach has a major shortcoming. The valve command signals (x) that are obtained from building automation systems do not always

represent the physical positioning of the valve accurately. This is, in particular, the case when a valve experiences a slow opening or closing, but not oscillations.

It was argued by Song et al. (2013) that this mismatch could be the result of static and dynamic valve responses. To understand these responses, a few concepts should be described:

1. Static valve response: the difference between valve command and valve movement when the system is in a steady-state condition – this response is defined using the Valve Dead Band, which represents the amount of signal change required to reverse the valve direction.
2. Dynamic valve response: the difference between the input and output when the valve is already in motion – this response is defined using Hysteresis, which represents a path-dependent characteristic.

Other than the above responses, that are from valve itself, the mismatch between the actual valve position and the valve command can also be explained by the resolution of the valve actuating device, e.g. a valve actuator. The actuator resolution is the smallest possible movement that an actuator can initiate. If the actuator receives a valve command for a valve movement smaller than the actuator resolution, the actuator is not capable of moving the valve stem to make the movement. All the factors, including valve responses and actuator resolution, contribute the mismatch between the actual valve position and valve commend and it becomes accumulatively large when the valve is moving rather slowly. This is evident in an actual experiment that is reported in Shahahmadi and Song (2018). The reported mismatch is illustrated in Figure 2.1.

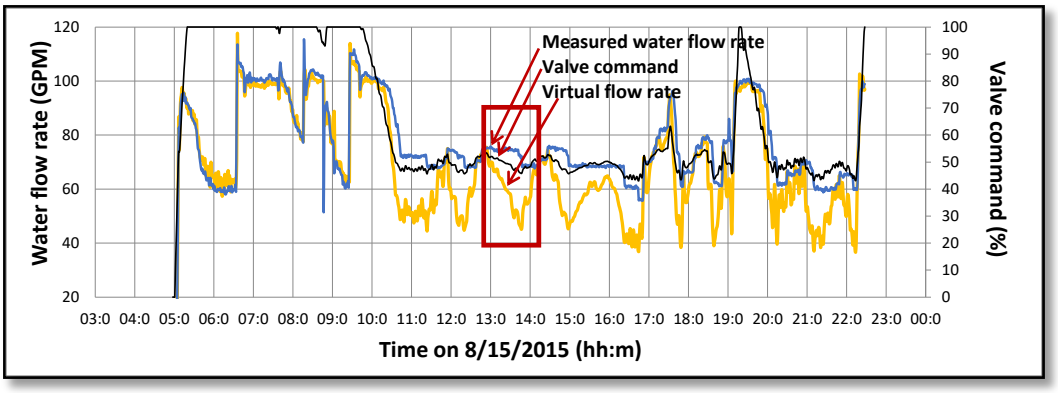

Figure 2.1.: The mismatch of valve command and valve positions.

The above figure shows that in the early hours of this experiment (i.e., 5:00-11:00) large changes in the valve position were introduced through major changes in valve command. In those hours, virtual and actual flow rate are quite comparable. In fact, the virtual measurement follows the actual measurement of flow rate rather closely. In the hours that follow (i.e., 11:00-19:00), valve commands experienced slow changes, which lead to no responses in valve position. During that time period, it is evident that the virtual flow rate expressed large deviations from the actual flow rate. Almost always, the virtual rate (yellow plot) is less than the actual rate (blue plot). This experimental evidence could support the proposed effects of static and dynamic valve responses, as described in Song et al. (2013). In order to make sure that no physical malfunction is causing the difference in this experiment, the valve commands are drastically changed again during the hours that follow (i.e., 19:00-20:00). As expected, the virtual flow rate follows the measured rate closely during that hour. In short, the static and dynamic valve responses and experimental evidence suggest that the virtual flow rate measurement may not be an accurate measurement for the actual flow rate when valve command remains relatively small changes. That introduces a major challenge to the usage of the virtual flow rate

measurement. This mismatch can be explained by stiction and deadband depending on the valve moving conditions.

1. Static friction

Static friction is, in particular, responsible for the mismatch of a stagnant valve, which is also knowns as Stiction. *"[T]he resistance to the start of motion"*, the Instrument Society of America (ISA) describes stiction, *"[could be] measured as the difference between the driving values required to overcome static friction upscale and downscale*'' (ISA Subcommittee SP75.05, 1979). In this context, when changes in valve command signal are small (e.g., from 11:00 to 19:00 in Figure 2.1), the valve may not overcome the static friction in the system, limiting the required changes in position. In that case valve command may not represent the actual valve position, which may cause a problem in virtual flow measurement.

As pointed out by Kano et al. (2004), this is also a common phenomenon in pneumatic valves that typically operate by air or gas under pressure. The valve position in pneumatic devices may remain intact, until the controller output overcomes stiction. Then, the position changes suddenly when the difference between elastic forces and air pressure is greater than the stiction in the system.

Chudhury et al. (2008, P.145) suggests that the term stiction has been used in the literature over the last fifty years, and it has in fact been examined widely. Considering the context of this research, recent studies on valve stiction often take empirical approaches. Some recent studies also rely on simulation results or physical models. Jalili and Huang (2010) offered a detailed survey of the existing literature on stiction detection and diagnosis. Horch (1999), for instance, introduced

a method by which one can distinguish between external oscillating disturbances and stiction in control valves using the cross-correlation between controller output and process output.

Further, there are two other contributions in this line of literature that are closely related to each other. Chudhury et al. (2005) employed data analysis and simulation tools to understand the causes of valve stiction with deterministic input signals. Given the difficulties of theoretical modeling of valve stiction, they took an empirical approach in their study. Against this background, another model for valve stiction was introduced by Kano et al. (2004), who improved the model developed by Chudhury et al. (2005) by incorporating deterministic and stochastic input signals. In Kano et al. (2004), the stiction forces were detected using two alternative methods. First, when the valve position does not change following a change in controller output, stiction could be detected, especially when such sections last long enough. Second, neglecting the slip-jumps, the relationship between the valve position and controller output, which tends to be like a parallelogram, could be used to detect stiction.

2. Deadband

The mismatch between virtual measurement of flow rates and the actual flow rates could also be due to the presence of deadband. As its name would suggest, deadband refers to "*a range through which an input signal may be varied […] without initiating an observable change in output signal*" (Chudhury et al. 2005, P. 643). In this case, the actual valve position (output) may remain stationary

up to the point that the net applied force becomes large enough, despite the fact that the valve command (input) indicates a change in position.

Such phenomenon could, in practice, generate a phase lag between valve command and valve position. This may impose a problem beyond the static resistance to the valve motion. Therefore, relying on observed input and output information in the presence of deadband may lead to an error in measurement. In particular, this happens when we rely on virtual measurement without taking the valve behavior into account.

In HVAC applications, Song et al. (2013) point out that, at a fixed valve position, the actual opening of a control valve varies depending on whether the valve is opening or closing. This suggests that there is a need to incorporate the *dynamic* behavior of the valve into virtual measurement to improve its precision. Given this dynamic behavior, we could examine "*the difference between the input and output when the valve is in motion*" (Song et al. 2013, P. 336).

Knowing the causes of the above mismatch, we can predict the valve position by employing the information about the valve command and by incorporating the information about deadband and sticition. This empirical correction eliminates the need for any further valve control data, including the valve feedback signal data. It also enables us to improve the precision of virtual flow meter.

Given the above definitions, two corrections are needed for converting commands to actual positions:

1. Despite the changes in input, when the valve is stagnant, the position of the valve should stay the same when the control inputs are not large enough to overcome the stiction (actuator resolution included).
2. When the valve is in motion and the valve input signal changes in the same opening or closing direction, the valve position should remain unchanged when the signal change is not significant enough to overcome the deadband.
3. When the valve is in motion and the valve input signal changing direction (i.e., from closing to opening or vice versa), the valve position should remain unchanged when the signal change is not significant enough to overcome the hysteresis, which consists of deadband, backlash and etc.

To make this correction, either simulation tools are used, or empirical approaches are taken. Among the first empirical papers in this line, one may refer to Horch (1999). His study was focused on setting apart the external oscillating disturbances and the stiction in control valves. For this purpose, the correlation information between the controller and process output was employed in order to identify the reason for oscillation.

Choudhury et al. (2005) is also among the key studies in modeling stiction in control valves. Using a mechanistic model of stiction and real-life industrial data, a model for stiction was developed in their study. This model was also improved in Kano et al. (2004). In their study, both deterministic and stochastic input signals were examined.

After an exhaustive review of different commonly used terms such as deadband, hysteresis, and stiction, Choudhury et al. (2005) provided some

industrial examples for stiction at power plants, petroleum refineries, and furnace. A physical model of valve sticition was, then, described in their paper. Given that the parameters of this model were unknown, they simulated the model outcome by imposing common parameter values. They also used the plant data, taking a data-driven approach, in order to identify the valve siciton in their model. The key parameters in their data-driven approach included the sum of deadband and stickband and slip-jump as illustrated in Figure 2.2. below.

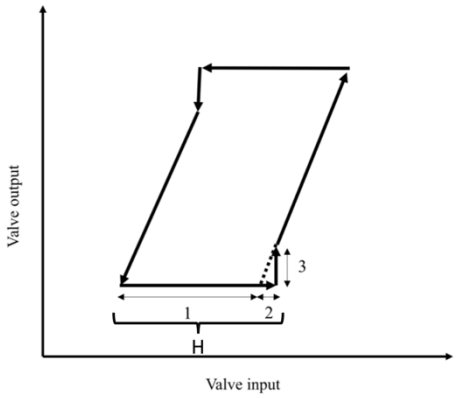

Figure 2.2: Typical input-output behavior of a sticky valve (Choudhury et al., 2005)

(Note – 1: deadband, 2: stickband, and 3: slip-jump.)

Choudhury et al. (2005) made use of an algorithm to identify the cases when the valve was stuck. This algorithm also enabled them to identify the stick positions. Under this method, the valve starts moving when the cumulative changes of input signal exceed the sum of deadband and stickband. Also, in case the input signal does not change direction, the valve starts moving when the cumulative changes of input signal exceed stickband. Given this information, the valve output is identified as the difference between input and a secondary term, which is a function of deadband, stickband, and slip-jump. This algorithm was, then, modified by Kano et al. (2004) in order to allow for the possibility of input signal being stochastic.

The above method may be of use in manufacturing plants where control devices have great computational capacities. As mentioned above, these methods are in fact tested in petroleum refineries with advanced manufacturing devices. The building automation systems, however, may severely lack such computational capacities. Therefore, a simplification is required.

In addition to the deadband, hyteresis and stiction, the valve mechanical behaviors, the valve actuator control resolution also impacts the mismatch between the valve commands and valve positions as explained earlier.

2.3. An Empirical Approach to the Mismatch Detection Using Building Automation Systems

A simplified algorithm for the mismatch detection is introduced in Shahahmadi and Song (2018). This algorithm is offered, given the computational capacities of control devices that are used in medical, commercial, academic, or residential buildings. The ultimate purpose of this algorithm is to correct valve commands into valve positions that could eventually be used in virtual flow measurement. There are five important variables in this algorithm: the valve command, previous stuck position, hysteresis, stiction and resolution errors, and min/max value for valve command. The above variables are listed and noted in Table 2.1. The algorithm in use is also visualized in Figure 2.2.

Table 2.1: The key variables in modified algorithm.

Variable	Definition
X(k)	Valve command
X(ss)	Previous stuck position
H	Hysteresis
S	Stiction and resolution errors
Y(k)	Minimum valve command value (0) Maximum valve command value (100)

As described in Shahahmadi and Song (2018), the first step of the modified approach is to compare the current valve command signal with the previous signal. This is done to determine the slope of the valve command changes; i.e., whether increasing, decreasing, or staying the same. This is noted by *Sign* in Figure 2.2.

At the next stage, the slope function output is defined as:

- +1 if the slope is positive: valve opening
- -1 if the slope is negative: valve closing

Any change in the slope denotes an instance when the valve changes directions. At each instance, the valve command is compared with the previous stuck position (noted as Xss). Once the difference between the two becomes greater than a certain threshold, the valve slips and starts moving.

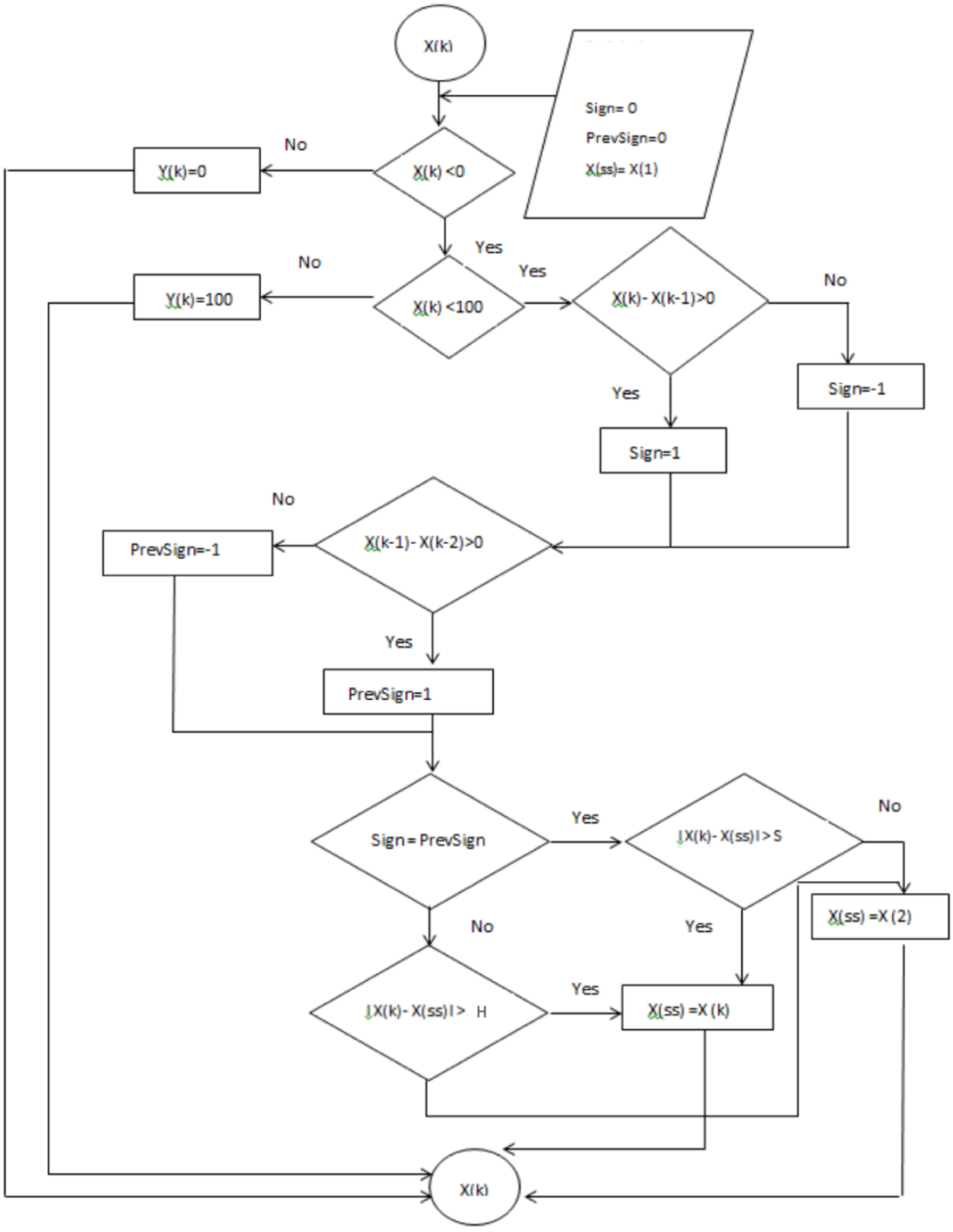

Figure 2.3.: Flow chart of correcting valve commands into valve positions.

The slip threshold is one of two values and depends upon whether a valve experiences any changes in direction. If the valve is reversing direction (the slope having changed from +1 to -1 or vice versa), the slip threshold is equal to the valve hysteresis. In other words, when the valve changes direction, the cumulative changes in the command signal compared with Xss must overcome deadband plus

stiction and backlash before the valve actually moves. However, if the valve still maintains the same direction, the slip threshold is only equal to the stiction, deadband and resolution errors, donated by S. In other words, if the valve movement comes to a rest and then starts again in the same direction (without reversing direction), the cumulative changes in the command signal compared with Xss must overcome S value before the valve starts moving.

The slope direction of the command at the moment of valve sticking must always be considered and compared with the slope of the command at every moment while the valve is stuck. If the slope was +1 at the moment of sticking, then any change in the slope to -1 while the valve is stuck sets the slip threshold to H. The slip threshold is only set to S if the valve never tries to reverse direction from becoming stuck to slipping. The new calculated valve position remains the same while the valve is stuck, and changes when the valve slips and starts moving.

As can be seen, S and H are two different thresholds that need to be identified in order to correct the valve commands into the valve positions. An empirical method is introduced in Shahahmadi and Song (2018) that could be used to obtain the values for S and H.

In Choudhury et al. (2005) and Kano et al. (2004), a range of parameters have been assigned to S and H. In Shahahmadi and Song (2018), however, in-situ measurements were conducted in order to determine the thresholds. In the measurements, very small incremental changes were manually made (via valve command overrides) and the actual valve position was closely monitored for any changes at the same time.

Two types of valve command overrides are introduced:

1. In order to identify the thresholds, i.e., the number of command changes that cause the position change, the valve overrides need to be done in the same direction and in the reverse direction

2. In order to understand whether the threshold values remained constant throughout the range of valve movement, the valve overrides are repeated for low, medium, and high ranges of valve commands.

The empirical method was implemented in a test valve. The test valve served as a control valve on a cooling coil in an air-handling unit. For this experiment, a data logger and a laptop computer that can be connected to the building automation system were used. The data logger was used to log valve positions signals and valve command signals, and the computer was used to override the valve. The valve was then overridden under three conditions, where valve command ranges are set to be equal to:

- 10%-20%: low range
- 50%-60%: medium range
- 90%-100%: high range

Then, a series of 0.1 percentage point incremental increases in valve command was introduced. Within windows of 30 seconds, valve positions were then monitored and tracked using loggers. Under each condition (low, medium, or high ranges), the above steps were repeated in descending order, where valve commands were lowered in 0.1 percentage point increments.

Under the assumptions about the range of valve commands, valve positions, indicating by valve feedback signals, are observed. Then, given the observed empirical relationship between valve command and valve position, the values for stiction and hysteresis could be identified. Considering the computational capacities of building automation systems, this approach will be tested in next chapters.

Chapter 3: Valve Flow Meter Enhancement Through Computing Valve Dynamic Behavior: The Empirical Findings

In this chapter, an experimental set-up is described, and a number of experiments are conducted on two air handling units (AHU) in a medical facility in Oklahoma City, OK, USA. The experimental design and data collections were done in 2016 and 2017. The set-up and the obtained data would enable us to empirically measure the improvements in virtual valve meters, employing the methods that were fully described in Chapter 2. By exploring the improvements in two AHUs, we are able to offer more details about the mechanism by which the corrected valve commands could help us in improving virtual meters.

In what follows, our findings for the smaller AHU, which will be referred to as AHU13 (given the on-site specifications), are described in Section 3.1. Then, our findings for the larger AHU, which will be referred to as AHU2 (given the on-site specifications), are described in Section 3.2. Lastly, the findings are compared, and conclusions are drawn in Section 3.3.

3.1. Empirical Findings Using the Data from a Relatively Small Air Handling Unit (AHU13)

In this section, we rely on the data obtained from a particular AHU, which is installed in a medical facility, in order to assess the improvements in virtual flow meters that are used for valves. The test AHU distributes conditioned air to office and pharmacy spaces. The schematic of the AHU13 is shown in Figure 3.1. The test AHU has both a cooling coil and heating coil. The design information for this AHU is given in Table 3.1. The cooling capacity of the AHU is 119.33 MBH

(34972.17 W) and the design chilled water flow rate through the valve is 23.9 GPM (0.001508 m^3/s).

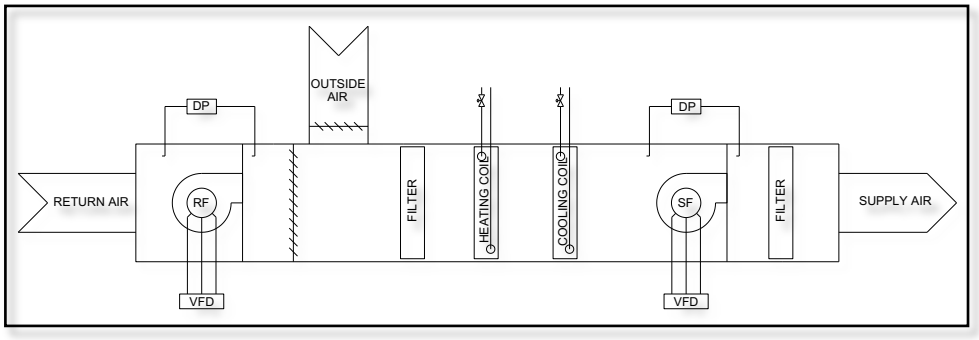

Figure 3.1: Selected AHU basic schematic.

Table 3.1: Design Information for AHU13.

Cooling Coil	Capacity	119.333 MBH (34972.17 W)
	Water Flow	23.9 GPM (0.001508 m^3/s)
	Pipe Size	2 inch (5.08 cm)
	Coil DP	10 ft of water (4.33 psi)
	Valve Size	3/4inch (1.905 cm)
	Valve Cv	10
	Valve DP	13.133 ft of water (5.69 psi)

The main objective of this test is to assess the improvements in virtual flow meters that are used for valves using the data that are obtained from a relatively small AHU. As discussed in previous chapters, stiction and deadband prevent the valve from moving until a set of certain thresholds is met. Identifying those specific threshold values are an empirical matter. That is why a particular experimental method is developed in order to obtain the values for S and H.

The stiction curves for varying ranges of valve command overrides are first introduced for a relatively small AHU. Given the average S and H in each range, a new command is computed. This new command is then compared with the original command and the actual position of the valve. The valve command is then plotted

to visualize the expected bias that may exist in observations and computations. The required corrections in the computed valve commands are then conducted using our findings about the values for two thresholds as well as an empirical valve characteristic curve. In order to draw a conclusion, the calculated flow rate using valve commands, calculated flow rate using valve positions, measured flow rate by the ultrasonic meter, and calculated flow rate using corrected valve commands are compared and uncertainty analyses are conducted.

3.1.1. Obtaining Stiction (S) and Hysteresis *(H)*

In previous studies, typically a range of parameters are assigned to S and H. Examples include Choudhury et al. (2005) and Kano et al. (2004). In more recent studies, however, in-situ measurements are conducted. An example includes Shahahmadi and Song (2018). These measurements are done in order to determine the thresholds. To do so, incremental changes are manually made via valve command overrides, while the actual valve position is closely monitored.

In order to identify the number of command changes that cause a change in position, the valve overrides need to be done in the same direction and in the reverse direction. Also, the valve overrides are repeated for low, medium, and high ranges of valve commands in order to observe whether the threshold values are kept constant throughout the range of valve movement.

Experimenting with the smaller AHU, the valve is overridden under three conditions:

1. Low Range: valve command ranges are set to be equal to 10%-20%
2. Medium Range: valve command ranges are set to be equal to 50%-60%

3. High Range: valve command ranges are set to be equal to 90%-100%

Then, a series of 0.1 percentage point incremental increases in valve command is introduced. Within windows of 30 seconds, valve positions are monitored and tracked using loggers.

As shown in Figure 3.2, the valve is first overridden under the low range of valve command: between 10% and 20%. Incremental changes in valve commands are then introduced, first with increasing valve commands and then with declining valve commands.

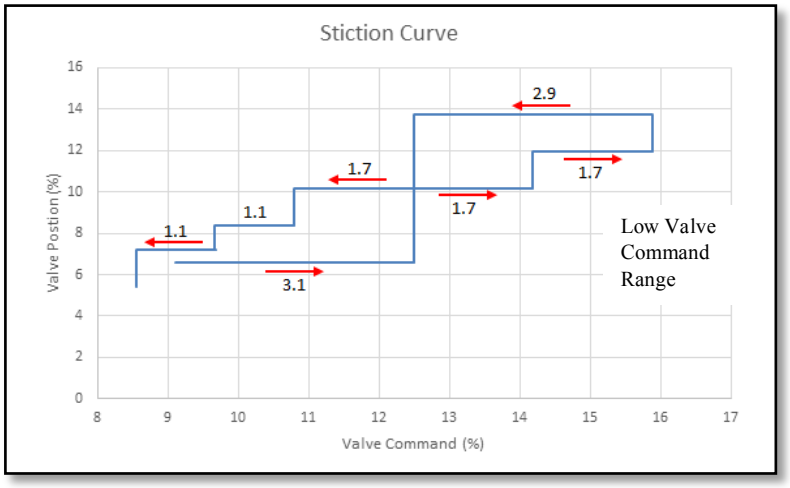

Figure 3.2: Changes in valve position following changes in valve command under low valve command ranges (10%-20%).

As illustrated in Figure 3.2, there were initially no significant changes in valve position. The valve position stayed the same (at about 6.5%), while the valve command increased from 10% to 12.5%. As proposed in Shahahmadi and Song (2018), the different values between the valve commands and positions imply that there exists a constant magnitude bias in measurements. In fact, different values for the same command may be generated by the internal signal converters used in the

valve actuator and the building automation system. Such bias could also be detected when the newly improved valve command and positions were compared.

As valve command exceeded 12.5%, a significant increase was observed in valve position. In this case, valve position increased from 6.5% to slightly above 10%. The valve position remained the same after that, until the valve command exceeds 14.25%. At that level, the valve position increased to 12%. Eventually, when the valve command exceeded 15.75%, the valve position increased to slightly less than 14 %.

Following the increase in valve position, which is a result of increase in valve command, the process was reversed, and the valve command was reduced incrementally. Upon the reduction in valve command, the valve position increased. The valve command continued to decline. As it declined from about 15.75% to 12.5%., the valve position remained intact (at about 14%). When the valve command went back to 12.5%, the valve position declined to 10%. This remained the same until the valve command was lowered to 10.75%, when the valve position dropped to slightly above 8%. The average thresholds with and without a direction change were 1.7% to 3.0%, respectively.

The second range required valve commands to be between 50% and 60% (medium range). Similar to the pattern that emerged for low range valve commands, the valve position increased under medium range conditions when incremental increases in valve command were introduced, and the magnitude of those changes was in a similar range to the changes that occurred in the low range. This was also the case when changes in valve commands were reversed, shown in Figure 3.3.

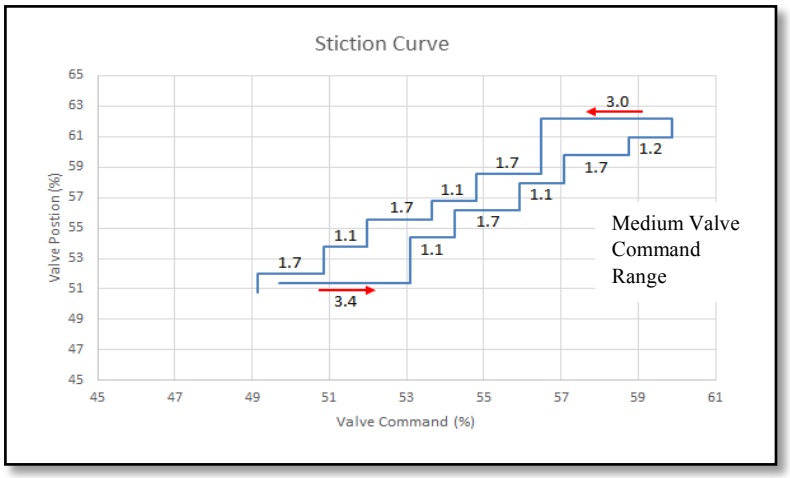

Figure 3.3: Changes in valve position following changes in valve command under medium valve command ranges (50%-60%).

The third range required valve commands to be between 90% and 100% (high range). The emerging pattern was similar to low and medium range variations. The magnitude of changes was comparable to the low range case and to the medium range case. This is illustrated in Figure 3.4.

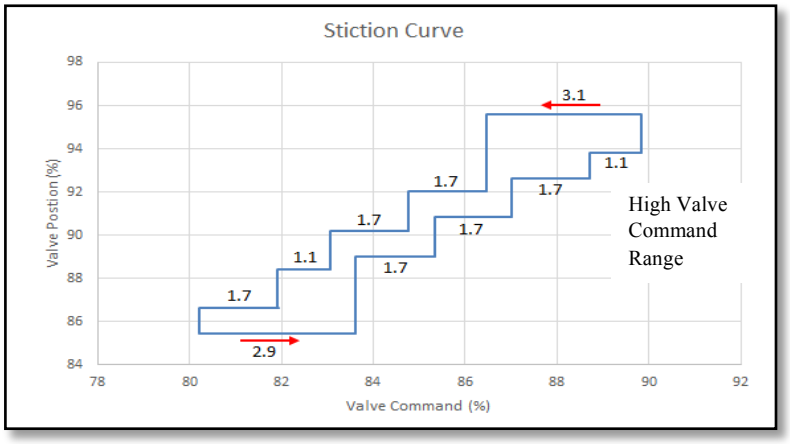

Figure 3.4: Changes in valve position following changes in valve command under high valve command ranges (90%-100%).

The average S and H from all three range cases are used to validate the flow chart presented in the algorithm discussed in Chapter 2. The results are shown in Figure 3.5. Incorporating S and H, the corrected command is closer to the actual

position. However, as described above, there is a constant bias caused by the different signal conversion factors, which can be eliminated by the different valve curve coefficients in the virtual valve meter implementation in the next section.

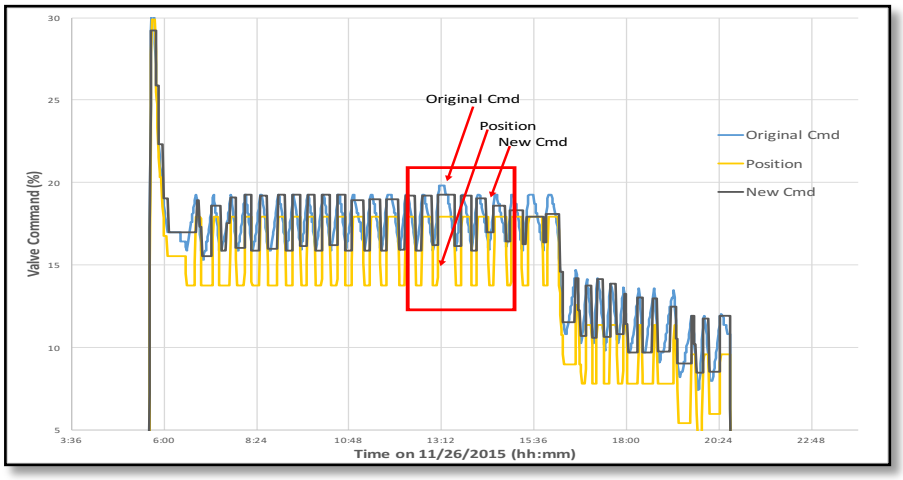

Figure 3.5: The valve corrected command, original command, and valve positions.

3.1.2. Valve Characteristics Curve

As discussed in Chapter 2, the calculation of the valve characteristics curve is done using the formula below:

$$f(x) = \frac{Q}{\sqrt{\Delta P}} \tag{3}$$

where Q is used for measured water flow and ΔP is used for differential pressure at different valve positions. Given the values for measured water flow rate and differential pressure, $f_v(x)$ could be computed to identify the installed valve characteristics curve for the observed valve command x.

The $f(x)$ curve is obtained by overriding the valve command at every 10% interval, starting from 0% opening to 100% opening. The valve was kept at the

same position for 15 minutes in order to eliminate the first two transient points at each interval. The water flow rate (Q) and differential pressure (ΔP) at each valve position were recorded and averaged after taking out the transient points. The correlation between the computed *f(x)* values and the valve position data is then regressed using a sixth order polynomial equation, implying that the regressed *f(x)* curve is a valve characteristic curve for steady-state valve operations.

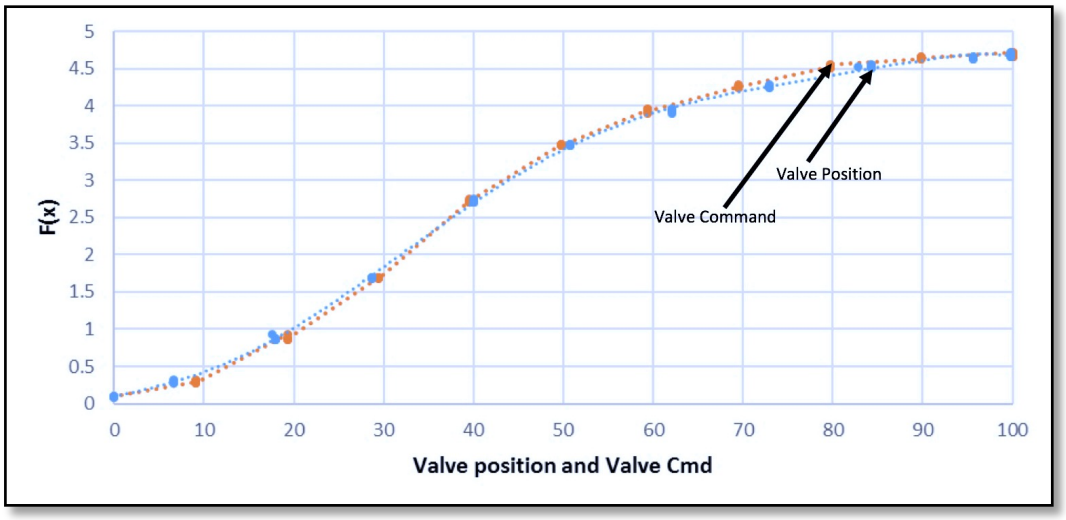

Figure 3.6: Valve performance characteristic curves.

For this computation, the average differential pressure (noted as *Average DP*), average valve command (noted as *Average Command*), and average valve position command (noted as *Average Position*) are computed using a dataset that was gathered in November 2015 at a medical facility in Oklahoma City, OK, USA. The collected dataset also includes the data for water flow rate. Given the above averages, re-scaling is done using some common conversions to convert the electric signals to the physical values for each measured variable, as described by Equations 4 through 6. These equations yield the converted average differential pressure

(noted as *Converted DP*), the converted average valve command (noted as *Converted Command*), and the converted average valve position (noted as *Converted Position*). The calculations are as follows:

$$ConvertedDP = 25 \times [(AverageDP - 1)/(5 - 1)] \quad (4)$$

$$ConvertedCommand = 100 - [100 \times (\frac{AverageCommand - 1.766}{10 - 1.766})] \quad (5)$$

$$ConvertedPosition = 100 - [100 \times \left(\frac{AveragePosition - 2}{8}\right)] \quad (6)$$

Introducing an override (from 0% to 100% and then from 100% back to 0%), the data for differential pressures, command, position, and flow rate are collected to compute the empirical valve characteristics curve using the max-operation below:

$$f(x) = \frac{Q}{\sqrt{P}} = MAX(\frac{FlowRate}{\sqrt{DP}}, 0) \quad (7)$$

Given the above information and calculation, valve command and valve position are plotted in Figure 3.6.

The regressed *f(x)* curve is a valve characteristic curve for steady-state valve operations. Employing the empirical coefficients obtained in Figure 3.6, a virtual water flow rate was then computed. Figure 3.7 compares the different flow rates obtained by the ultrasonic meter and calculated by the valve commands and corrected commands.

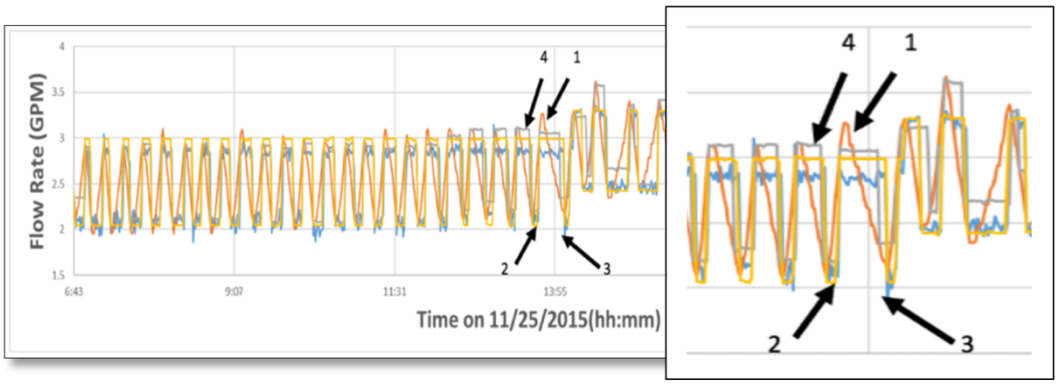

Figure 3.7: Comparison between the measured flow rates, calculated flow rates using valve commands, and calculated flow rates using corrected commands.

(Notes – 1: calculated flow using valve commands; 2: calculated flow rate using valve positions; 3: measured flow rate by the ultrasonic meter; 4: calculated flow using corrected valve commands.)

The differences between the calibrated flow rates using commands, corrected commands, and the actual flow rates recorded by the ultrasonic meter were then computed. In particular, in order to evaluate the performance of different flow calculations, three sets of errors were compared:

1. $Error_1$ – the absolute error between measured flow rate (V_U), which was measured by the ultrasonic meter, and the calculated flow rate (V_C), which was calculated using the corrected valve command, is taken for the first set of errors.
2. $Error_2$ – the absolute error between the measured flow rate (V_U) and the calculated flow rate using the valve original command (V_O), which was not corrected for, is taken for the second set of errors.
3. $Error_3$ – the absolute error between the measured flow rate (V_U) and valve position flow rate (V_P) is taken for the third set of errors.

The corrected valve command was used in V_C, but the observed valve command with no correction was used for V_O. For V_P, valve position flow rate is used. Below, the mean and standard deviation of the above errors are reported.

The mean of the absolute error between V_U and V_C (i.e. mean of $Error_1$) is equal to 0.14 GPM (8.83×10^{-6} m^3/s), with standard deviation being 0.18 GPM (1.13×10^{-5} m^3/s), while the mean of the absolute error between V_U and V_O (i.e. mean of $Error_2$) is equal to 0.30 GPM (1.89×10^{-5} m^3/s), with standard deviation being 0.25 GPM (1.58×10^{-5} m^3/s). Also, the mean of the absolute error between V_U and V_P (i.e. mean of $Error_3$) is equal to 0.10 GPM (6.31×10^{-6} m^3/s), with standard deviation being 0.11 GPM (6.94×10^{-6} m^3/s).

Also, errors are compared in relative terms, as given in Equations 8-10. The mean for the first set of relative errors, calculated by the flow rate using corrected valve commands, is 7.26%, with standard deviation being 15.43%, while the mean for the second set of relative errors, calculated by the flow rate using the valve command without corrections, is 13.73%, with standard deviation being 16.34%. As can be seen, the relative error of the virtual flow rate has improved from 13.73% to 7.26% through introducing corrected valve commands. It is noted that, the mean for the third set of relative errors, calculated using the valve position, shows the best results, 5.8%, with standard deviation being 14.86%, but it is close to the first set of relative error.

Lastly, in order to understand the error magnitude over the full range of the flow rate, the errors also compared with design flow rate of cooling coil (23.9 GPM

or 0.001508 m^3/s), as given in Table 3.1. For this case the following errors are defined:

$$Normzalized\ Error\ Over\ Design\ Flowratae_1 = \frac{|V_U - V_C|}{V_d} \quad (8)$$

$$Normzalized\ Error\ Over\ Design\ Flowratae_2 = \frac{|V_U - V_O|}{V_d} \quad (9)$$

$$Normzalized\ Error\ Over\ Design\ Flowratae_3 = \frac{|V_U - V_P|}{V_d} \quad (10)$$

where V_U, V_C, V_O, and V_P are defined as above, and the denominator (V_d) is the design flow rate. The mean for the first set of normalized error is 0.58%, with standard deviation being 0.75%, while the mean for the second set of normalized error is 1.26%, with standard deviation being 1.04%. As can be seen, the normalized error of the virtual flow rate, when compared to the design flow rate, has improved from 1.26% to 0.58% through introducing corrected valve commands. However, both errors are shown to be acceptable using the percentage over full range due to the fact that the experiments were conducted at low flow rate seasons. Also, the mean for the third set of relative error design again shows the best result, 0.41% with standard deviation being 0.44%, which however is close to the results obtained used by the corrected valve commands. The absolute, relative and normalized errors are summarized in Table 3.2.

Table 3.2.: Absolute and Relative Errors (AHU13)

	Mean	*SD*
$Error_1=\|V_U-V_C\|$	0.14 GPM (8.83×10^{-6} m^3/s)	0.18 GPM (1.13×10^{-5} m^3/s)
Relative $Error_1=(\|V_U-V_C\|)/V_U$	7.26%	15.43%
Normalized Error Over $Design_1=(\|V_U-V_C\|)/V_d$	0.58%	0.75%
$Error_2= \|V_U-V_O\|$	0.30 GPM (1.89×10^{-5} m^3/s)	0.25 GPM (1.58×10^{-5} m^3/s)
Relative $Error_2=(\|V_U-V_O\|)/V_U$	13.73%	16.34%
Normalized Error Over $Design_2=(\|V_U-V_O\|)/V_d$	1.26%	1.04%
$Error_3=\|V_U-V_P\|$	0.10 GPM (6.31×10^{-6} m^3/s)	0.11 GPM (6.94×10^{-6} m^3/s)
Relative $Error_3=(\|V_U-V_P\|)/V_U$	5.8%	14.86%
Normalized Error Over $Design_3=(\|V_U-V_P\|)/V_d$	0.41%	0.44%

3.2. *Empirical Findings Using the Data from a Relatively Large Air Handling Unit (AHU2)*

In this section, we rely on the data obtained from a larger unit, which is installed in the same medical facility. The schematic of the AHU is shown in Figure 3.8. The test AHU has both a cooling coil and heating coil. The design information for this AHU is given in Table 3.3. The cooling capacity of the AHU is 608 MBH (178187 W) and the design chilled water flow rate through the valve is 101 GPM (0.0063721098 m^3/s).

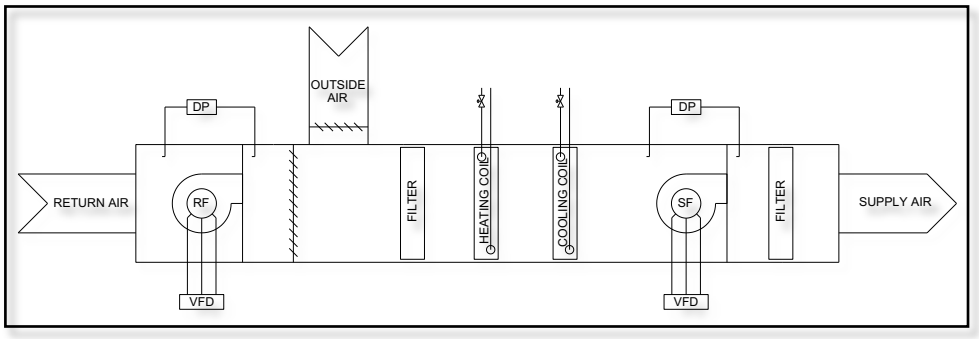

Figure 3.8: Selected AHU basic schematic.

Table 3.3: Design Information for AHU2

Cooling Coil	Capacity	608 MBH (178187 W)
	Water Flow	101 GPM (0.0063721098 m^3/s)
	Pipe Size	3 inch (7.62 cm)
	Coil DP	14.6 ft of water (6.32950 psi)
	Valve Size	2 inch (5.08 cm)
	Valve Cv	40
	Valve DP	14.674 ft of water (6.36158 psi)

3.2.1. Obtaining Stiction (S) and Slip-Jump (J)

As in Section 3.1.1, the valve overrides are provided in the same direction and in the reverse direction. The valve overrides are also repeated for low, medium, and high ranges of valve commands in order to observe whether the threshold values are kept constant or not.

As before, the valve was overridden under three conditions:

1. Low Range: valve command ranges are set to be equal to 10%-20%
2. Medium Range: valve commands ranges are set to be equal to 50%-60%
3. High Range: valve commands ranges are set to be equal to 80%-90%

Then, a series of 0.1 percentage point incremental increases in valve command was introduced. Within windows of 30 seconds, valve positions were then monitored and tracked using loggers.

Under each range (low, medium, or high), the above steps are repeated in descending order, where valve commands were lowered in 0.1 percentage point increments. Keeping the valve command at low ranges (10%-20%), Figure 3.9

illustrates the above steps for the increases and decreases in valve commands and the subsequent changes in valve position.

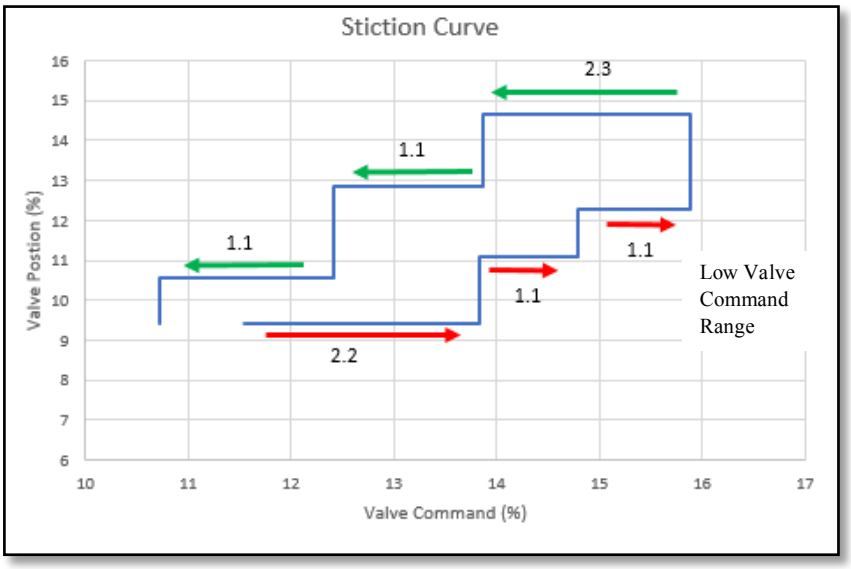

Figure 3.9: Changes in valve position following changes in valve command under low valve command ranges (10%-20%).

Following an increase in valve command (from less than 12% to about 14%), the valve is stuck at a particular position, which is slightly greater than 9%. In this range, the deadband plus stiction (J) value is computed to be about 2.2. The valve position changes as valve command approaches 14%. The new valve position is at 11%. The new valve position remains the same as valve command increases from 14% to about 15%. At this point, the stiction value (S) is 1.1. The valve position changes again as valve command approaches 15%. The new valve position is slightly above 12%. The new valve position remains the same as valve command increases from 15% to about 16%. At this point, the stiction value is again 1.1.

The valve command is then changed in descending order. While the command is reduced from about 16% back to 14%, the valve position is stuck at a

value slightly less than 15%. The deadband plus stiction (J) value is computed to be equal to 2.3. The valve command is reduced even further all the way back to 11%. The valve position declines to about 13% and 11%. During these changes, the stiction value is computed to be about 1.1.

A similar pattern is observed when we examine the changes in medium and high range. Given the changes in valve commands and valve positions, as illustrated in Figures 3.10 and 3.11, the deadband plus stiction (J) value and stiction values are computed.

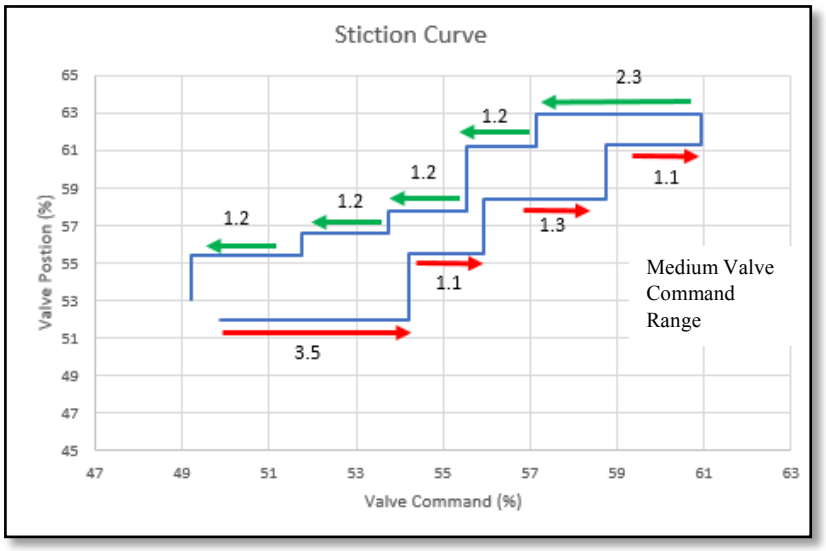

Figure 3.10: Changes in valve position following changes in valve command under medium valve command ranges (50%-60%).

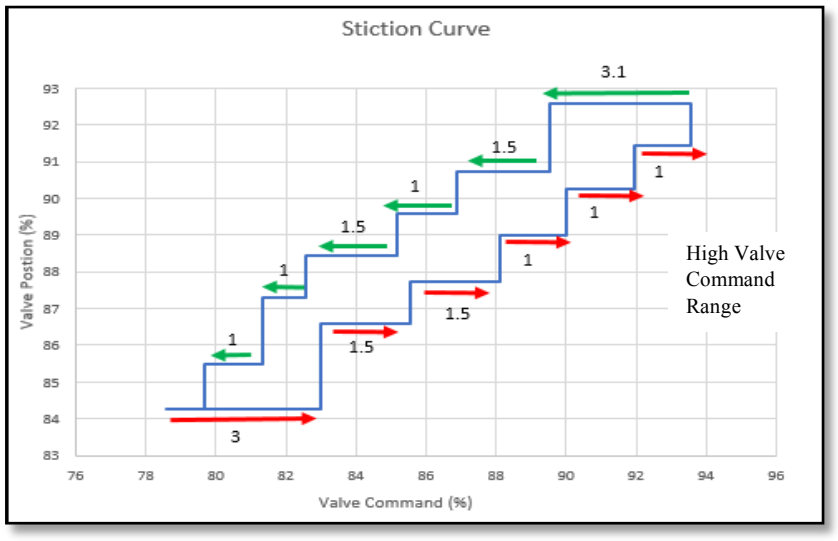

Figure 3.11: Changes in valve position following changes in valve command under high valve command ranges (10%-20%).

3.2.2. Valve Characteristics Curve

Similar to Section 3.2.2., the valve characteristics curve is obtained by overriding the valve command at every 10% interval, starting from 0% opening to 100% opening. The valve was kept at the same position for 15 minutes in order to eliminate the first two transient points at each interval. The water flow rate (Q) and differential pressure (ΔP) at each valve position were recorded and averaged after taking out the transient points. The correlation between the computed *f(x)* values and the valve position data is then regressed using a sixth order polynomial equation, implying that the regressed *f(x)* curve is a valve characteristic curve for steady-state valve operations. The obtained valve characteristic curves are shown in Figures 3.12-1 to 3.12-6.

For this computation, the *Average DP*, *Average Command*, *Average Position* are computed using a dataset that was gathered in September and August

of 2017 at a medical facility in Oklahoma City, OK, USA. This is a same medical facility as described in Section 3.1. Like above, the collected dataset also includes the data for water flow rate. Given the above averages, re-scaling is done using some common conversions, as described by Equations 2 through 4, in order to obtain the *Converted DP*, *Converted Command*), and *Converted Position*). Introducing an override (from 0% to 100% and then from 100% back to 0%), the data for differential pressures, command, position, and flow rate are collected to compute the empirical valve characteristics curve using the max-operation that was introduced in Equation 5.

Given the above information and calculation, valve command and valve position are plotted for ascending and descending overrides in Figures 3.12-1 to 3.12-6. The plots are organized for valve commands (Figures 3.12-1 to 3.12-3) and for position (Figures 3.12-4 to 3.12-6).

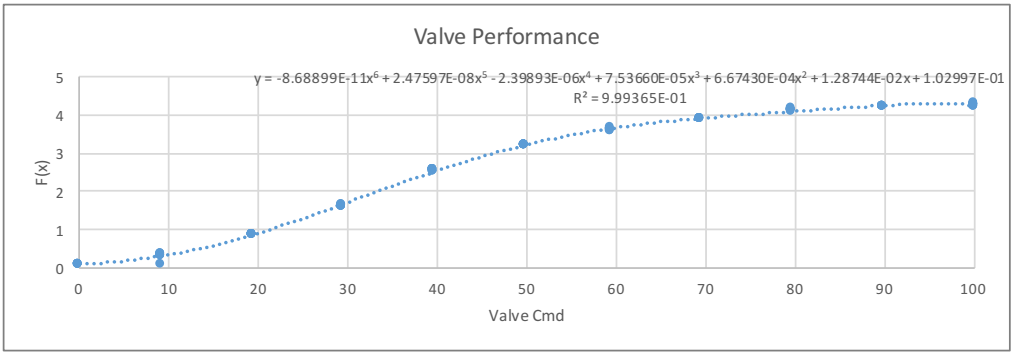

Figure 3.12-1: Valve Command for Ascending Override

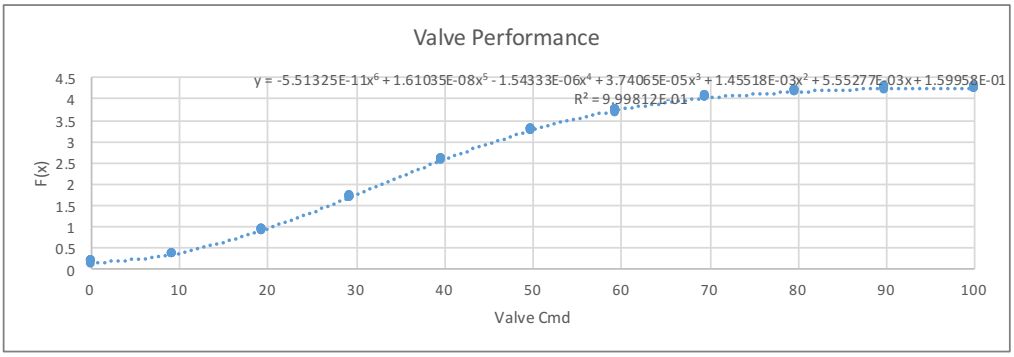

Figure 3.12-2: Valve Command for Descending Override

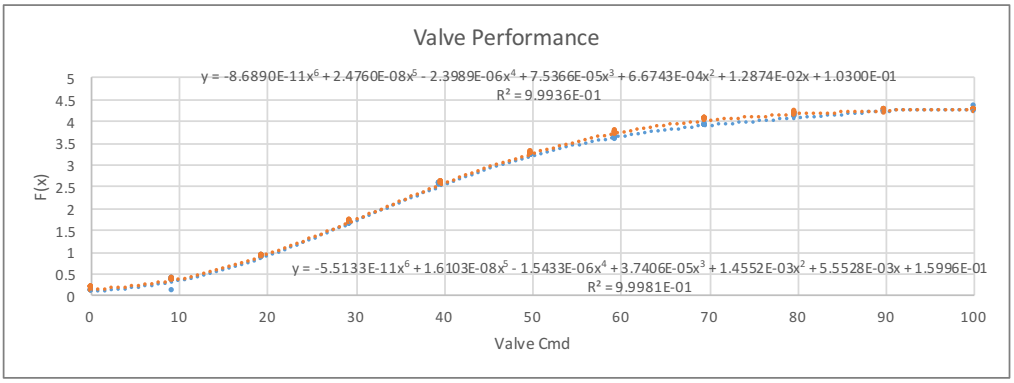

Figure 3.12-3: Combination of Figure 3.12-1 and 12-2

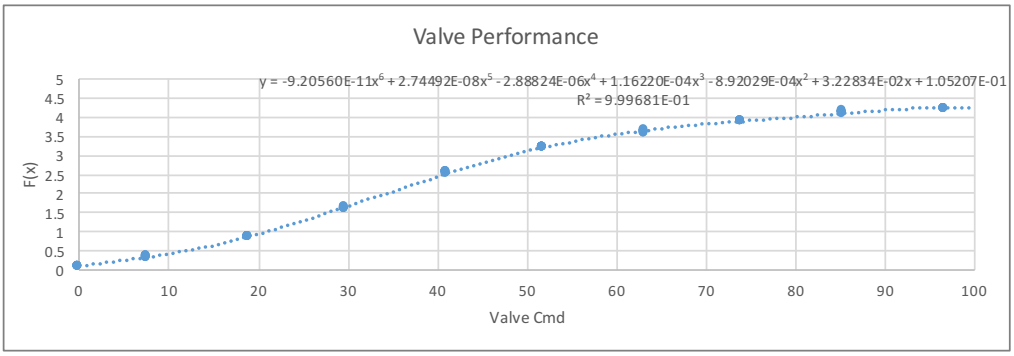

Figure 3.12-4: Valve Position for Ascending Override

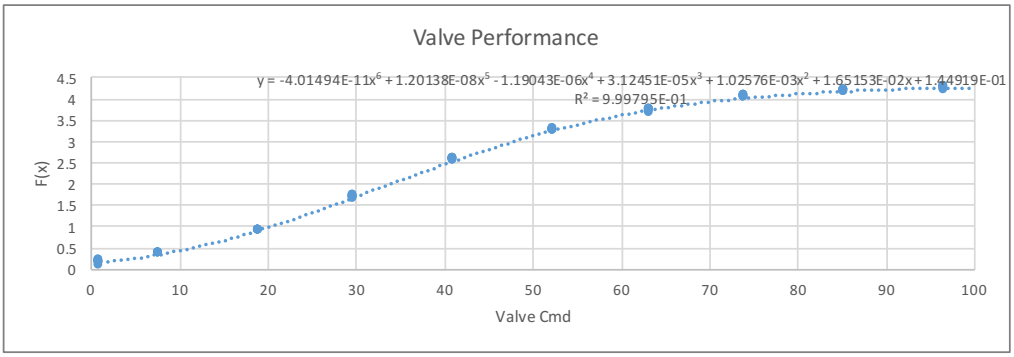

Figure 3.12-5: Valve Position for Descending Override

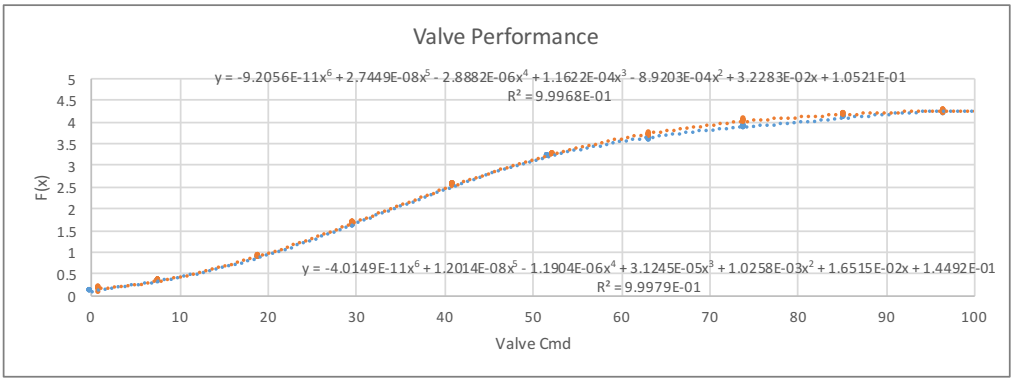

Figure 3.12-6: Combination of Figure 3.12-4 and 12-5

Using the information that are provided in the above figures, the ultimate valve characteristic curve is put together in Figure 3.13. In this figure, the valve characteristic curve is drawn twice, once as a function of valve command and once as a function of valve position.

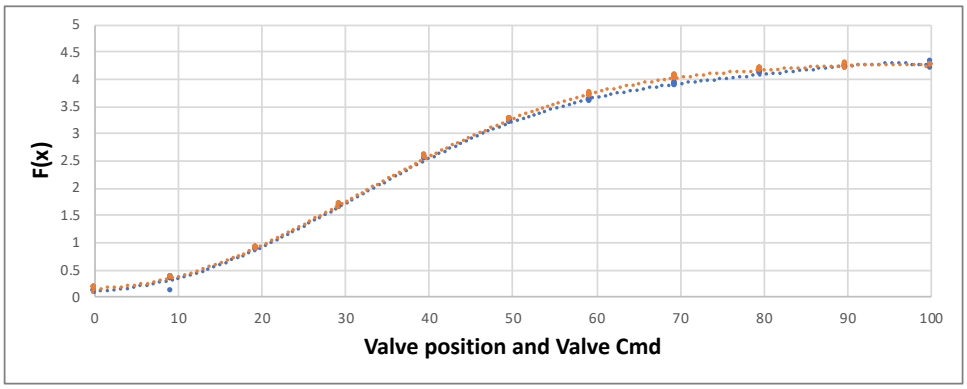

Figure 3.13: Valve characteristic cure (AHU2)

The valve characteristic curve in Figure 3.13 is for steady-state valve operations. Using the obtained coefficients, a virtual water flow is then computed. Figure 3.14 compares the different flow rates that are obtained by the ultrasonic meter and calculated by the valve commands and corrected commands.

Figure 3.14: Comparison between ultrasonic flow rate, valve command flow rate, corrected valve command flow rate, and valve position flow rate

Given different types of flow rates that are available at this point, a formal comparison could be made to evaluate how close the virtual flow measurement is to the observed flow. For this, a set of three errors, similar to the errors in Section 3.1, are defined:

1. *Error$_1$* – the absolute error between measured flow rate (V_U), which was measured by the ultrasonic meter, and the calculated flow rate (V_C), which was calculated using the corrected valve command, is taken for the first set of errors.
2. *Error$_2$* – the absolute error between the measured flow rate (V_U) and the calculated flow rate using the valve original command (V_O), which was not corrected for, is taken for the second set of errors.
3. *Error$_3$* – the absolute error between the measured flow rate (V_U) and valve position flow rate (V_P) is taken for the third set of errors.

The corrected valve command was used in V_C, but the observed valve command with no correction was used for V_O. For V_P, valve position flow rate is used. Below, the mean and standard deviation of the above errors are reported. The mean of the absolute error between V_U and V_C (i.e. mean of $Error_1$) is equal to 0.56 GPM (3.53304E-5 m^3/s), with standard deviation being 0.36 GPM (2.27124E-5 m^3/s), while the mean of the absolute error between V_U and V_O (i.e. mean of $Error_2$) is equal to 1.01 GPM (6.37209E-5 m^3/s), with standard deviation being 0.83 GPM (5.23647E-5 m^3/s). Also, the mean of the absolute error between V_U and V_P (i.e. mean of $Error_3$) is equal to 1.13 GPM (7.12917E-5 m^3/s), with standard deviation being 0.73 GPM (4.60557E-5 m^3/s). Alternatively, errors are compared in relative terms, as given by Equations 7, 8, and 9. For this case, the following errors are defined. The mean for the first set of relative errors, calculated by the flow rate using corrected valve commands, is 5.40%, with standard deviation being 3.77%, while the mean for the second set of relative errors, calculated by the flow rate using

the valve command without corrections, is 9.91%, with standard deviation being 8.91%. As can be seen, the relative error of the virtual flow rate has improved from 9.91% to 5.40% through introducing corrected valve commands.

Table 3.4: Absolute and Relative Errors (AHU2)

	Mean	*SD*
$Error_1=\|V_U-V_C\|$	0.56 GPM (3.53304E-5 m^3/s)	0.36 GPM (2.27124E-5 m^3/s)
Relative $Error_1=(\|V_U-V_C\|)/V_U$	5.40%	3.76%
Normalized Error Over $Design_1=(\|V_U-V_C\|)/V_d$	0.55%	0.35%
$Error_2= \|V_U-V_O\|$	1.01 GPM (6.37209E-5 m^3/s)	0.83 GPM (5.23647E-5 m^3/s)
Relative $Error_2=(\|V_U-V_O\|)/V_U$	9.91%	8.91%
Normalized Error Over $Design_2=(\|V_U-V_O\|)/V_d$	1%	0.82%
$Error_3=\|V_U-V_P\|$	1.13 GPM (7.12917E-5 m^3/s)	0.73 GPM (4.60557E-5 m^3/s)
Relative $Error_3=(\|V_U-V_P\|)/V_U$	10.81%	7.53%
Normalized Error Over $Design_3=(\|V_U-V_P\|)/V_d$	1.12%	0.72%

3.3. Summary of Findings

The findings that are reported in Sections 3.1 and 3.2 suggest that virtual flow measurement could be quite precise; in particular, when the dynamic behavior of valve is taken into account. This is, in fact, evident in small AHUs (Section 3.1) and large AHUs (Section 3.2).

Compared to flow rates that are computed based on valve command or valve position, the corrected virtually measured flow rates are much closer to the observed flow rates using ultrasonic. This is well-reflected in the comparison that are made in absolute errors and relative errors. More precisely, in both small and large AHUs, the average of the absolute value of the difference between the

corrected flow and the ultrasonic flow is less than the average of the absolute value of the difference between the flow that is computed based on valve command or position and the measured flow rate. This is also the case in relative errors. These could all be taken as evidence for the usefulness of virtual flow measurement when the dynamic behavior of the valve is fully taken into account.

Chapter 4: The Application of the Virtual Flow Meter in Monitoring the Performance of Air Handling Units

Monitoring the performance of air handling units (henceforth, AHU), which under certain circumstances may lead to significant energy savings, is among the key applications of virtual flow meters. As discussed in Chapter 2, physical sensors that are typically installed in ducts or pipes usually disrupt the flow rate. As a result of that, the proper measurement of flow rates become almost impossible. They are also quite costly, and they require large spare spaces. Lastly, as argued by Andiroglu (2015) and Wang et al. (2014), the flow rate may be affected by other factors such as fan head and fan motor power. Given these practical benefits, different usages of virtual valve flow meters in energy consumption management of HVAC systems have recently become widespread.

In fact, many scholarly efforts have been undertaken over the last twenty years to propose effective control system adjustments that could potentially reduce energy consumption in HVAC systems and improve their efficiency. Simulation studies in this line of literature include Mathews et al. (2000, 2001, and 2002), which are based on a series of changes in control systems (including reset control, economizer control, setback control, fan control, etc.). It also includes a study by Fong et al. (2006), in which evolutionary control methods are utilized. Other than simulation studies, there have been multiple empirical efforts in improving energy efficiency of HVAC systems. Among those, one could refer to Canbay et al. (2004), Markis and Paravantis (2007), and Escrivá-Escrivá et al. (2010).

As highlighted in Cho and Liu (2009), the settings of Variable Air Volume (henceforth, VAV) could be of vital importance for energy consumptions in AHUs. Thus, it is very important to monitor such settings. In doing so, as applied in Shahahmadi, Rivas, Song, and Wang (2017), virtual flow measurements are proved to be quite useful. In particular, virtual flow meters could be used in monitoring the reset of the minimum airflow of VAVs in order to find the optimal minimum air flow for an efficient use of energy in AHUs.

In this chapter a summary of the research by Shahahmadi, Rivas, Song, and Wang (2017) is provided. In this study, the AHUs that are used in medical facilities are examined. These facilities usually require higher minimum airflow ratios for more stringent air ventilation controls. However, there are still significant energy savings opportunities by customizing the minimum airflow ratio settings by different zone functionalities and different occupancy schedules.

In this study, a case study medical building is used to demonstrate the energy savings potential by implementing a custom set of minimum airflow ratio settings. Four minimum airflow setting measures are implemented:

1. During occupied hours, the minimum airflow for non-critical zones is set equal to 30% of maximum airflow. This is fully monitored using virtual flow measurement.
2. During unoccupied hours, the minimum airflow for non-critical zones is set equal to zero CFM. This is also monitored by a virtual flow meter.
3. During occupied and unoccupied hours, the minimum airflow is set equal to zero CFM for interior rooms that are in non-critical zones.

4. The setting for critical zones remains intact.

Taking these measures, energy consumption is well-managed as outside air temperature increases. In fact, experimental evidence suggests that, with an increase in outside air temperature (from about 50 ºF to 80 ºF), energy consumption is controlled significantly following the implementation of the above changes. This is illustrated in Figure 4.1. This graph shows the variations in outside air temperature on the horizontal axis (in Fahrenheit) and cooling energy levels on the vertical axis (in KBtu/hr), obtained by the virtual chilled water flow rate measurements multiplied by the temperature differences between the supply and return water. As outside air temperature increases from 51ºF to 79ºF, cooling energy consumption increases much more when the above measures are not taken. However, the energy consumption is curbed successfully as outside temperature increases once the above improvements are introduced to the system.

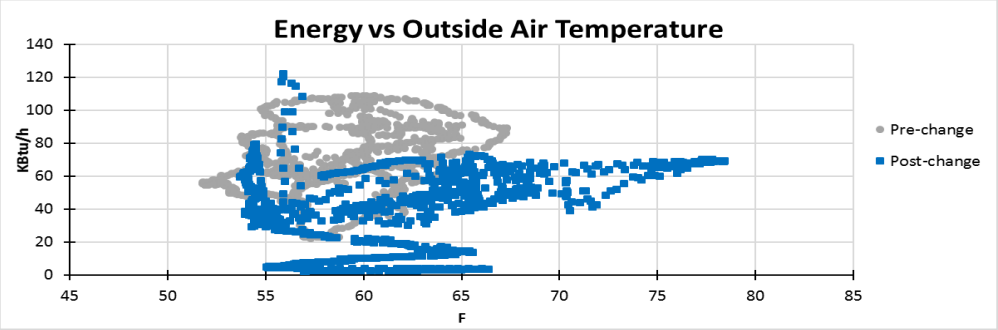

Figure 4.1: Energy vs. outside air temperature.

A key element in this experiment is the use of virtual flow measurement. In particular, virtual flow meters are used to measure chilled water flow rate through the cooling coil, which in turn is used in computing cooling energy consumption.

In what follows, the HVAC systems that are installed in this medical facility are described in Section 4.1. Then, improvements that are introduced in the control system are discussed in Section 4.2. Resulting energy savings are also described in Section 4.3.

4.1. The Installed HVAC System

The medical building that is examined in this study is located in Oklahoma City, OK, and it includes 10 non-critical AHUs (e.g., office space) and 3 critical AHUs. The critical units are used for dentistry, surgical, and pharmacy services. The minimum airflow was initially set to be equal to around 80% of total airflow in all VAVs. Also, there were five different types of air exchange rates in this facility. This was not necessary, however, as most of the units on site are not critical. In fact, only three critical units are used for medical purposes such as surgery, pharmacy, and dentistry.

With no detailed analyses, one major flaw is observed in the installed HVAC system: the minimum airflow for other non-critical units should not have been set at the same level as for critical units. There are also some interior spaces on site that do not have any windows, and yet minimum airflow had been set as for critical units. Such set-up may lead to inefficient use of energy, which motivates the changes that are introduced to the system.

Table 4.1 below summarizes the total airflow rate for critical and non-critical VAVs, their percentage in the facility, and their relative importance. It also

offers more details about the maximum airflows for critical and non-critical zones for each AHU.

Table 4.1. Airflow Rates for Non-critical and Critical VAVs

No.	*Airflow rate*	*Non-critical VAVs*			*Critical VAVs*		
	CFM	*No.*	*Sum of Dsg. CFM*	*Percentage*	*No.*	*Sum of Dsg. CFM*	*Percentage*
AHU1	6185.37	11	6185.37	100	0	0	0
AHU2	10264.23	25	10264.2	100	0	0	0
AHU3	11914.96	33	11915	100	0	0	0
AHU4	13063.58	2	673.83	5.16	42	12389.75	94.84
AHU5	7727.88	17	4856.68	62.85	15	2871.20	37.15
AHU6	11196.56	15	5850.44	52.25	23	5346.12	47.75
AHU7	12459.43	27	9204.73	73.88	9	3254.70	26.12
AHU8	18160.68	15	4919.31	27.09	34	13241.37	72.91
AHU9	9453.11	27	9253.93	97.89	1	199.18	2.11
AHU10	12352.12	23	8399.73	68.00	16	3952.39	32.00
AHU11	13905.38	24	6830.4	49.12	23	7074.98	50.88
AHU12	29877.32	8	29877.3	100	0	0	0
AHU13	2371.41	8	2371.41	100	0	0	0
Sum	158932	235	110602		163	48329.69	

4.2. Improvements in Control Systems

As mentioned above, the first improvement has to do with a reduction in airflow for VAVs in non-critical exterior zones. Recent revisions to ASHRAE Standard 90.1 are applied in this case, which leads to a reduction to 30% of maximum airflow rate for the VAVs that serve non-critical exterior zones. Figure 4.2 illustrates this reduction during the occupied hours.

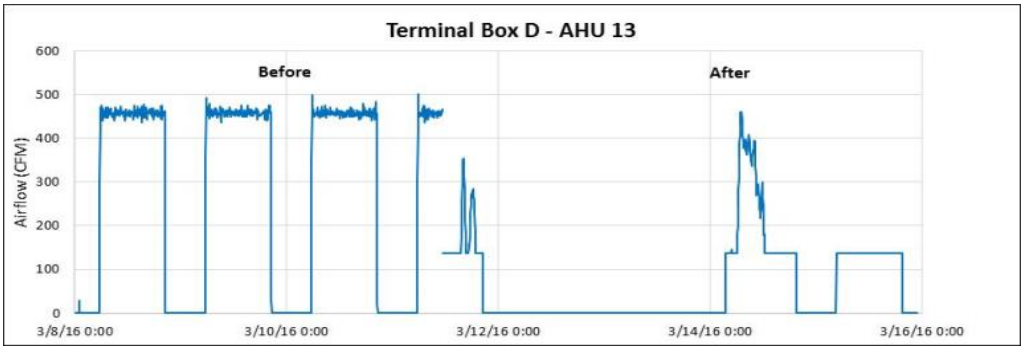

Figure 4.2: Reduction in airflow following the recent revisions to ASHRAE Standard 90.1

The second improvement sets the minimum airflow equal to 0% during unoccupied hours. Like the first improvement, this change may lower the energy consumption. Figure 4.3 shows minimum airflow, the actual airflow, and box flow during two working days (from 11 a.m. on the first day to 5:45 p.m. on the second day). In this example, the minimum airflow during occupied hours (from 11 a.m. to 7 p.m. on the first day and from 5:45 a.m. to 5:45 p.m. on the second day) is set to be equal to 43 CFM, which is 30% of the maximum airflow rate following the first improvement. Also, the minimum airflow during unoccupied hours (from 7 p.m. on the first day to 5:45 a.m. on the second day) is set to be equal to 0 CFM.

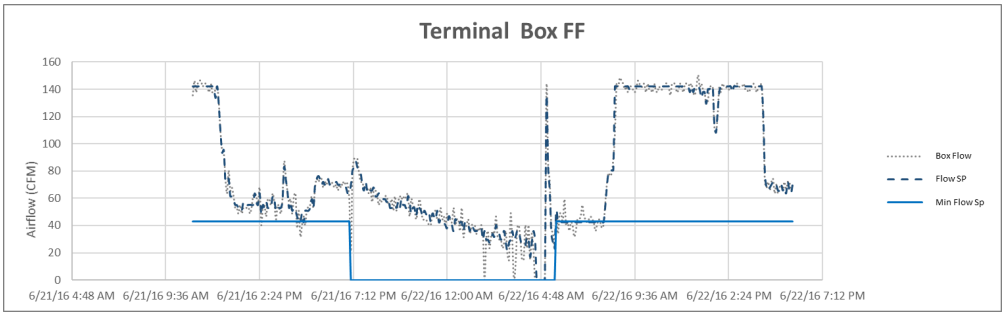

Figure 4.3: Setting the minimum airflow based on the revisions to ASHRAE Standard 90.1 during occupied hours and 0 CFM during occupied hours.

The third improvement sets the minimum airflow equal to 0% for the interior rooms with no windows for all non-critical zones. This is done since these rooms are not exposed to heat transfer through exterior surfaces due to temperature differences or sun light. The only causes for cooling load are occupancy and equipment use in the rooms. During occupied and unoccupied hours, the minimum airflow in the interior rooms is set to be equal to 0 CFM with the expectation that the airflow rate will be sufficiently supplied due to the cooling load generated by occupant once the room is occupied. Figure 4.4 shows the adjustments in actual airflow as a result of setting minimum airflow equal to 0 CFM for the interior rooms with no windows for all non-critical zones. As evident in Figure 4.4, although the minimum airflow ratio is set to zero, the actual airflow rate has been always significantly higher especially during occupied hours.

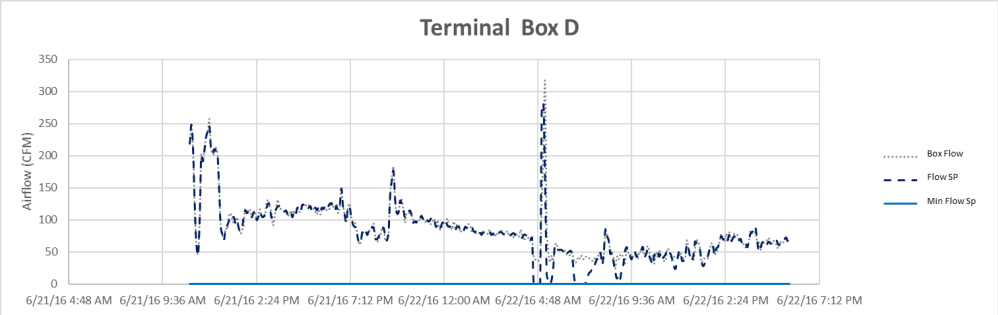

Figure 4.4: Setting minimum airflow equal to 0 CFM for the rooms with no windows.

Lastly, minimum airflow rate is kept intact for critical units during occupied hours to avoid any potential problems in personnel performance. The actual flow rate, however, may change during the unoccupied hours. This is illustrated in Figure 4.5. This figure shows the minimum airflow rate, the actual airflow rate, and the box flow rate for a critical unit over a two-day period.

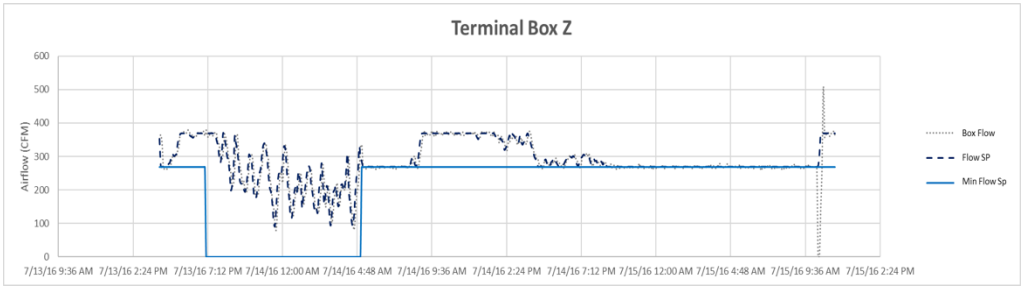

Figure 4.5: Imposing no minimum airflow for critical units.

Two points must be highlighted. First, since these improvements are introduced to the HVAC systems of a medical facility, a few adjustments are made. Given the importance, the use, and the size of the rooms, for instance, the minimum flow rate is revised for all the units. This includes more than 350 VAV boxes. To illustrate this better, two different rooms could be considered. In a room that is being used for examination, the airflow rate is set at the higher value when the required flow rate is compared to the one offered by the revisions to ASHRAE Standard 90.1. In contrast, the minimum airflow rate is reduced to 30%, as proposed by recent revisions to ASHRAE Standard 90.1, in an office that is not used for examination.

The second point, which relates more directly to the discussions in Chapters 1, 2, and 3, is that in these improvements virtual flow measurement is used to monitor the cooling energy use in the cooling coil, which is impacted directly by the reheats of the VAVs. This was advantageous to this experiment, as it made it less costly, more space-efficient, and much more precise. Plus, the usage of virtual flow meters enabled us to take into account other factors that may affect the flow (e.g., Andiroglu 2015 and Wang et al. 2014).

4.3. Energy Savings

Taking the above measures, energy consumption is significantly controlled as outside air temperature increases. As shown in Figure 4.1, cooling energy rarely reaches 75 KBtu/hr once the above changes are introduced, while cooling energy level reaches 110 KBtu/hr in the absence of the above changes. In particular, energy savings are evident when the temperature varies between 57.5ºF and 67.5ºF.

Changes in energy consumption varied across different units. The largest reduction was recorded to be about 90%. It should be noted that this reduction was recorded for one unit, which showed a reduction of 30% in supply fan speed (henceforth, SF speed) and 40% in supply airflow (henceforth, SA flow). The smallest reduction was recorded to be about 15%. This reduction was recorded for four units, which showed reductions in supply fan speed and supply airflow of less than or equal to 25%. Variations in the amount of energy savings and changes in supply fan speed and supply airflow are summarized in Table 4.2 and Figures 4.6-1 and 4.6-2.

Table 4.2.: Changes in SF Speed, SA Flow, and Cooling Energy Consumption for 13 AHUs

AHU No.	*SF Speed*	*SA Flow*	*Energy*
1	-50%	-40%	-20%
2	-25%	-25%	-25%
3	-70%	-75%	-60%
4	-8%	-10%	-35%
5	-17%	-17%	-45%
6	-25%	-15%	-15%
7	-15%	-25%	-15%
8	-30%	-40%	-90%
9	-25%	-15%	-20%
10	-25%	-15%	-15%
11	-25%	-15%	-15%
12	-50%	-40%	-50%
13	-50%	-40%	-50%

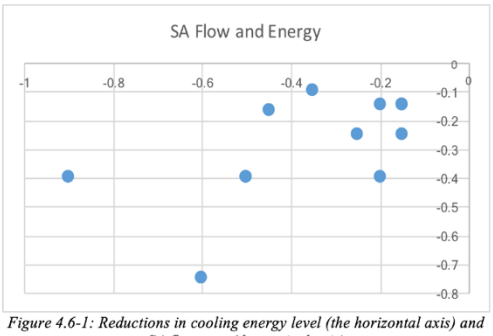

Figure 4.6-1: Reductions in cooling energy level (the horizontal axis) and SA flow rate (the vertical axis)

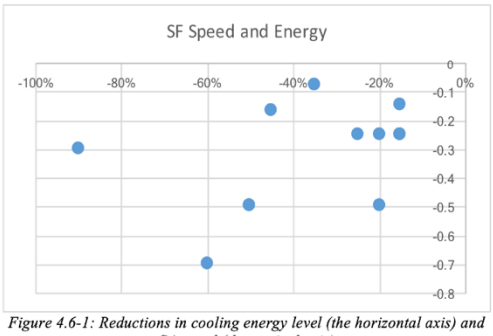

Figure 4.6-1: Reductions in cooling energy level (the horizontal axis) and SA speed (the vertical axis)

Using the virtual airflow measurements (not discussed in this thesis), it is shown in Figure 4.6-1 that following the proposed improvements units that experience greater reduction in SA flow rate tend to bring in more energy savings: generally speaking, a reduction in SA flow rate (vertical axis) leads to a decline in energy consumption (the horizontal axis). Also, it is shown in Figure 4.6-2 that following the proposed improvements units that experience greater reduction in SF speed tend to bring in more energy savings: generally speaking, a reduction in SF speed (vertical axis) leads to a decline in energy consumption (the horizontal axis).

More precisely, among the 13 units that are examined, seven units showed a reduction in energy that was less than or equal to 25%. Among them, only one unit showed reductions in supply fan speed and supply airflow that exceeded 25%. Also, four units showed a reduction in energy that was greater than 25% or equal to 50%. Among them, two units showed reductions in supply fan speed and supply air flow that were less than 25%. One unit, for which the reductions in supply fan speed and supply air flow were both greater than 50% or less than 75%, showed a reduction in energy that exceeded 50% but it was less than 75%. Lastly, another unit, for which the reductions in supply fan speed and supply airflow were both

greater than 25% and less than 50%, showed a reduction in energy that exceeded 75% but was less than 100%.

This experiment illustrates how useful virtual flow measurement could be in monitoring the VAVs settings. In particular, the virtual meters could efficiently be used for applying the requirements for the recent revisions to ASHRAE Standard 90.1, which as shown above may lead to a reduction in cooling energy consumption through a reduction in SF speed and SA flow rate.

Chapter 5: Conclusion

In this thesis, the effectiveness of virtual flow measurement in HVAC systems is examined. The findings suggest that virtual flow meters could be quite useful, effective, and precise, in particular when the dynamic behavior of valves are taken into account.

5.1. A Summary of Key Findings

In the above experiment, two sets of corrections are implemented to adjust for valve commands. Under these corrections, valve position is set to remain intact despite the fact that valve command changes. First, valve position is kept the same when control inputs are not large enough to overcome the stiction. Second, valve position is kept the same when changes in signals are not significant enough to overcome the deadband. These changes, however, could only be implemented when valve behavior is examined.

Under a careful treatment of valve dynamic behavior, virtual flow measurements could in general be as good as ultrasonic device measurements. Unlike physical flow meters, however, virtual flow meters are less expensive, more space-effective, and less disturbed by factors that are not controlled for in physical devices. Plus, the required computations could easily be conducted using the existing technologies in building automation systems.

To illustrate their effectiveness, this thesis also explores how recent revisions to some standard ASHRAE provisions may lower cooling energy consumption in contemporary HVAC systems that are used in medical facilities.

Using virtual measurements, adjustments in VAV settings are shown to be quite effective in reducing the supply fan speed and airflow, which then in turn leads to lower cooling energy consumption.

That said, the utilization of virtual flow measurement may go beyond the experimental designs for HVAC systems. They could also be used in other industrial set-ups. Examples include flow measurement in chemical plants (e.g., Choudhury et al. 2005) and petroleum industry (e.g., Faluomi et al. 2006, Bringedal and Phillips 2006, and Wang et al. 2014).

5.2. Future Research

Further research could improve our understanding of possible improvements in virtual flow measurements or their utilization. In particular, four topics should be highlighted. First, looking into other building facilities that may have different HVAC requirements could prove to be fruitful for further research. The current literature, as discussed in Chapter 2, is mostly focused on academic, medial, or residential facilities. However, other buildings like industrial or commercial facilities, hotels, or airports may have particular HVAC needs that are different from those in, say, medical facilities. Virtual flow measurement may be proved to be even more useful in those facilities.

Second, further examination of the effectiveness of virtual flow measurements in HVAC systems with varying sizes may also reveal some patterns that enable researchers to generalize their findings, so that they could be used in a more straightforward fashion in the industry. The literature is yet young, and

researchers have not been successful in conveying their findings to the industry. Such generalizations may make virtual measurement more accessible for HVAC industry.

Third, the usage of a device, rather than BAS, that could directly incorporate the estimated coefficients from each AHU's valve characteristic curve into the required computation for virtual flow measurement may help researchers to assess the performance of virtual flow measurement in larger scales. That technique may also become appealing to the industry.

Fourth, there might be factors other than the ones that are examined in this thesis (namely, the dynamic behavior of the valve) that may affect the precision of virtual flow measurement. Exploring those factors may also contribute to researchers' understanding of the usefulness of virtual measurements.

References

Andiroglu, E. (2015). *Development of virtual air / water flow meters using fan / pump head and motor power (Order No. 3719924)*. Available from ProQuest Dissertations & Theses Global. (1718418473). Retrieved from https://search-proquest-com.ezproxy.lib.ou.edu/docview/1718418473?accountid=12964

Andiroglu, E., Wang, G., Song, L., & Kiamehr, K. (2016). Development of a virtual pump water flow meter using power derived from comprehensive energy loss analysis. *Science and Technology for the Built Environment*, *22*(2), 214-226.

ASHRAE. (2013). ASHRAE fundamentals handbook, measurement and instruments, American Society of Heating, Refrigerating and Air-conditioning Engineers, Inc., Atlanta, GA.

Bringedal, B., & Phillips, A. (2006). Application of Virtual Flow Metering as a Backup or Alternative to Multiphase Flow Measuring Devices. In *Subsea Controls and Data Acquisition 2006: Controlling the Future Subsea*. Society of Underwater Technology.

Canbay, C. S., Hepbasli, A., & Gokcen, G. (2004). Evaluating performance indices of a shopping centre and implementing HVAC control principles to minimize energy usage. *Energy and Buildings*, *36*(6), 587-598.

Cheung, H., & Braun, J. E. (2014). Virtual power consumption and cooling capacity virtual sensors for rooftop units.

Cho, Y. H., & Liu, M. (2009). Minimum airflow reset of single duct VAV terminal boxes. *Building and Environment*, *44*(9), 1876-1885.

Choudhury, A. A. S., Shah, S. L., & Thornhill, N. F. (2008*). Diagnosis of process nonlinearities and valve stiction: data driven approaches*. Springer Science & Business Media.

Choudhury, M. S., Thornhill, N. F., & Shah, S. L. (2005). Modelling valve stiction. *Control Engineering Practice*, 13(5), 641-658.

Escrivá-Escrivá, G., Segura-Heras, I., & Alcázar-Ortega, M. (2010). Application of an energy management and control system to assess the potential of different control strategies in HVAC systems. *Energy and Buildings*, *42*(11), 2258-2267.

Faluomi, V., Dellarole, E., Bonuccelli, M., & Antico, L. (2006). Virtual metering system for oil and gas fields monitoring: design, implementation and applications. In *5th North American Conference on Multiphase Technology. BHR Group, Banff, Canada* (pp. 91-105).

Fong, K. F., Hanby, V. I., & Chow, T. T. (2006). HVAC system optimization for energy management by evolutionary programming. *Energy and Buildings*, *38*(3), 220-231.

Horch, A. (1999) A simple method for detection of stiction in control valves. *Control Engineering Practice*, 7(10), 1221-1231.

Huang, G., Wang, S., & Sun, Y. (2008). Enhancing the reliability of chiller control using fused measurement of building cooling load. *HVAC&R Research*, *14*(6), 941-958.

ISA Subcommittee SP75.05 (1979). Process instrumentation terminology. *Technical Report ANSI/ISA-S51*.1-1979. Instrument Society of America.

Jelali, M., & Huang, B. (Eds.). (2009). *Detection and diagnosis of stiction in control loops: state of the art and advanced methods*. Springer Science & Business Media.

Joo, I., Liu, M., Wang, J., & Hansen, K. (2003). Application of new technologies during continuous commissioning. In *Proceedings of International Conference on Enhanced Building Operation, Berkeley, CA*.

Kano, M., Maruta, H., Kugemoto, H., & Shimizu, K. (2004). *Practical model and detection algorithm for valve stiction*. In Proceedings of the Seventh IFAC-DYCOPS Symposium, Boston, USA.

Lee, P. S., & Dexter, A. L. (2005). A fuzzy sensor for measuring the mixed air temperature in air-handling units. *Measurement*, *37*(1), 83-93.

Markis, T., & Paravantis, J. A. (2007). Energy conservation in small enterprises. *Energy and Buildings*, *39*(4), 404-415.

Mathews, E. H., Arndt, D., & Geyser, M. F. (2002). Reducing the energy consumption of a conference centre—a case study using software. *Building and Environment*, *37*(4), 437-444.

Mathews, E. H., Arndt, D. C., Piani, C. B., & Van Heerden, E. (2000). Developing cost efficient control strategies to ensure optimal energy use and sufficient indoor comfort. *Applied Energy*, 66(2), 135-159.

Mathews, E. H., Botha, C. P., Arndt, D. C., & Malan, A. (2001). HVAC control strategies to enhance comfort and minimise energy usage. *Energy and buildings*, *33*(8), 853-863.

Mcdonald, E., Zmeureanu, R., & Giguère, D. (2014). Virtual flow meter for chilled water loops in existing buildings. In *Proc. Conf. eSim* (pp. 1-12).

Prieto, A. R., Thomas, W. M., Wang, G., & Song, L. (2017). In-situ fan curve calibration for virtual airflow sensor implementation in VAV systems. In *ASHRAE Transactions - ASHRAE Winter Conference* (Vol. 123, pp. 215-229).

Shahahmadi, S., Rivas, A., Song, L., & Wang, G. (2017) Energy Savings Potential in a Medical Facility through Custom Minimum Airflow Resets. In *AEI 2017* (pp. 419-431).

Shahahmadi, S. & Song, L. (2018) Valve Flow Meter Enhancement Through Computing Valve Dynamic Behaviors, *ASHRAE Transactions*, forthcoming.

Song, L., Wang, G., & Brambley, M. R. (2013). Uncertainty analysis for a virtual flow meter using an air-handling unit chilled water valve. *HVAC&R Research*, 19(3), 335-345.

Song, L., Joo, I. S., & Wang, G. (2012). Uncertainty analysis of a virtual water flow measurement in building energy consumption monitoring. *HVAC&R Research*, 18(5), 997-1010.

Wang, Z., Gong, J., Wu, H., & Li, Q. (2014). The Development and Application of Virtual Flow Metering System in Offshore Gas Field. In *2014 10th International Pipeline Conference* (pp. V001T09A019-V001T09A019). American Society of Mechanical Engineers.

Wang, G., Kiamehr, K., & Song, L. (2016). Development of a virtual pump water flow meter with a flow rate function of motor power and pump head. *Energy and Buildings*, *117*, 63-70.

Wang, G., Song, L., Andiroglu, E., & Shim, G. (2014). Investigations on a virtual airflow meter using projected motor and fan efficiencies. *HVAC&R Research*, *20*(2), 178-187.

Wichman, A., & Braun, J. E. (2009). A smart mixed-air temperature sensor. *HVAC&R Research*, *15*(1), 101-115.